

MICROCOPY RESOLUTION TEST CHART
NATIONAL BUREAU OF STANDARDS 1963-A

12



TR-0104

AD

Reports Control Symbol
OSD - 1366

**AN IMPROVED SMOKE OBSCURATION MODEL ACT II:
PART 1 THEORY**

ADA111922

JANUARY 1982

By

R. A. Sutherland

D. W. Hoock

FILE COPY

DTIC
ELECTE
MAR 11 1982
E

Approved for public release; distribution unlimited.



US Army Electronics Research and Development Command

Atmospheric Sciences Laboratory

White Sands Missile Range, NM 88002

82 00 11 063

NOTICES

Disclaimers

The findings in this report are not to be construed as an official Department of the Army position, unless so designated by other authorized documents.

The citation of trade names and names of manufacturers in this report is not to be construed as official Government indorsement or approval of commercial products or services referenced herein.

Disposition

Destroy this report when it is no longer needed. Do not return it to the originator.

REPORT DOCUMENTATION PAGE		READ INSTRUCTIONS BEFORE COMPLETING FORM
1. REPORT NUMBER ASL-TR-0104	2. GOVT ACCESSION NO.	3. RECIPIENT'S CATALOG NUMBER
4. TITLE (and Subtitle) AN IMPROVED SMOKE OBSCURATION MODEL ACT II: PART 1 THEORY		5. TYPE OF REPORT & PERIOD COVERED Final Report
		6. PERFORMING ORG. REPORT NUMBER
7. AUTHOR(s) R. A. Sutherland D. W. Hoock		8. CONTRACT OR GRANT NUMBER(s)
9. PERFORMING ORGANIZATION NAME AND ADDRESS US Army Atmospheric Sciences Laboratory White Sands Missile Range, NM 88002		10. PROGRAM ELEMENT, PROJECT, TASK AREA & WORK UNIT NUMBERS DA Task No. 1L161102B53A
11. CONTROLLING OFFICE NAME AND ADDRESS US Army Electronics Research and Development Command Adelphi, MD 20783		12. REPORT DATE January 1982
		13. NUMBER OF PAGES 65
14. MONITORING AGENCY NAME & ADDRESS (if different from Controlling Office)		15. SECURITY CLASS. (of this report) UNCLASSIFIED
		15a. DECLASSIFICATION/DOWNGRADING SCHEDULE
16. DISTRIBUTION STATEMENT (of this Report) Approved for public release; distribution unlimited.		
17. DISTRIBUTION STATEMENT (of the abstract entered in Block 20, if different from Report)		
18. SUPPLEMENTARY NOTES		
19. KEY WORDS (Continue on reverse side if necessary and identify by block number) Smoke obscuration modeling Thermal emission Propagation Transmission Contrast modeling Path radiance		
20. ABSTRACT (Continue on reverse side if necessary and identify by block number) This report describes the theoretical basis for the smoke obscuration model ACT II. The work encompasses analytical procedures for determining smoke concentration, temperature, path integrated concentration, path radiance, path luminance, target and background radiance, target-background luminance, and contrast transmission. The model includes both single scattering and thermal		

20. ABSTRACT (cont)

emission and is applicable for wavelengths from the visible through the infrared. Data from Smoke Week II are used to present an example of input/output.

CONTENTS

LIST OF TABLES.....	4
LIST OF FIGURES.....	5
1. INTRODUCTION.....	7
2. OUTLINE AND SCOPE.....	11
3. AMBIENT IRRADIANCE (SECTORING SCHEME).....	16
4. OPTICAL THICKNESS CALCULATIONS.....	18
5. CLOUD CONCENTRATION AND TEMPERATURE.....	20
5.1 Smoke Source Function (Q).....	21
5.2 Cloud Centroids (X, Y, and Z)	21
5.3 Dispersion Functions.....	22
5.4 Cloud Temperature and Buoyant Rise.....	23
6. EXAMPLE (FROM SMOKE WEEK II).....	25
6.1 Conversion of Model Results.....	25
6.2 Input Data.....	26
TABLES.....	29
FIGURES.....	32
REFERENCES.....	38

DTIC
COPY
INSPECTED
2

Accession For	
NTIS GRA&I	<input checked="" type="checkbox"/>
DTIC TAB	<input type="checkbox"/>
Unannounced	<input type="checkbox"/>
Justification	
By _____	
Distribution/	
Availability Codes	
Dist	Avail and/or Special
A	

LIST OF TABLES

1. Diffusion Parameters used in the Transport and Diffusion Routine for Various Values of Roughness Parameter (Z_0) and Stability Category.....	29
2. Ambient Radiation Measurements (Visible) from Smoke Week II, Trail 1 Field Test.....	30
3. Meteorological Inputs to the Model for Smoke Week II, Trial 1 Field Test.....	31

LIST OF FIGURES

1. Sketch demonstrating the effects of extinction and path radiance on radiant energy received by an observer.....	32
2. Sketch demonstrating the scattering of ambient radiation into the LOS.....	32
3. Sketch demonstrating the sky/terrain sectoring scheme used in the model.....	33
4. Sketch demonstrating the geometry for computing optical thickness.....	33
5. Photopic response curve and Gaussian functional fit for converting radiance (W/m^2) to luminance ($candles/m^2$).....	34
6. Test configuration for Smoke Week II, Trial 1 Field Test.....	35
7. Sky radiance map $W\ sr^{-1}\ m^{-2}$ as derived from Smoke Week II, Trial 1 Field Test.....	35
8. Model comparisons of path integrated concentration (CL) and path luminance with data from Smoke Week II, Trial 1 Field Test.....	36
9. Modeled diffuse and direct radiation as a function of target position along the LOS.....	37

1. INTRODUCTION

The Army inventory contains several models which compute transmission (T) through an obscuring medium composed, for example, of smoke or dust;¹ that is,

$$T = e^{-\tau} , \quad (1)$$

where τ is the optical depth along the path of propagation.

On one hand attempts are then made to directly relate transmission to electro-optical system performance and smoke effectiveness by considering only the directly transmitted signal:

$$S(\vec{r}) = S(\vec{r}_0)T , \quad (2)$$

where $S(\vec{r})$ is the optical signal received by an observer at (\vec{r}) from a target at \vec{r}_0 . The transmission (T) includes effects of both scattering out of the path plus absorption along the path, the composite process being referred to as extinction.

On the other hand system performance modelers know that electro-optical systems (including the eye-brain) respond not only to directly transmitted radiation but also to contrast, the definition of which may vary among models but generally requires an addition to equation (2) to account for path radiance, or "brightness." That is (see also figure 1),

$$S(\vec{r}) = S(\vec{r}_0)T + S_p(\vec{r}) , \quad (3)$$

where the contribution due to path radiance (S_p) may be due either to scattering of ambient radiation (for example, sun, moon, and sky) into the path of propagation or (thermal) emission along the path, or both. References to scattering out of and into are emphasized to note that the former does not directly contribute to path radiance and can usually be treated as indistinguishable from simple Beer's law attenuation. The latter however, which does contribute to path radiance, is usually a complex function of many factors, including angular properties of both the scattering medium and the ambient radiation.

¹R. A. Sutherland, D. W. Hooch, and R. B. Gomez, 1981, An Objective Summary of US Army Electro-Optical Modeling and Field Testing in an Obscuration Environment, ASL-TR-0096, US Army Atmospheric Sciences Laboratory, White Sands Missile Range, NM

Note that, unlike transmission, path radiance has a vector nature which means physically that in real world scenarios, such as the smoked battlefield, asymmetries exist between target and observer, giving one or the other an "optical advantage." This vector nature is the essence of the present model and should not be overlooked in the deceptively simple form of equation (3) or by the necessarily complex formulation to follow.

The existence of path radiance in real world scenarios is often of overriding significance in affecting perception and is commonly observed in nature. One example is the apparent disappearance of stars in daytime. Another is experienced by individuals driving a vehicle through fog with the headlights on high beam. In both cases perception is diminished due to interference caused by scattering that is manifested by path radiance. In the infrared the effect of path radiance is to (partially) offset the effects of absorption. Another example is radiance data sensed via orbiting satellites. Often such data are highly accurate ($\sim 1^\circ\text{C}$)^{2 3} when inverted to obtain surface temperature. This accuracy occurs despite the fact that the path transmission in these cases, even in the so-called atmospheric "windows," is only on the order of 60 percent, which if taken alone would imply a corresponding temperature error on the order of 50 to 100°C! The explanation here lies in the basic physics of infrared propagation in which, for practical scenarios, absorption is always accompanied by Kirchhoff (i.e., thermal) emission as elucidated for the case of the atmosphere in early works.^{4 5}

The degree to which scattering and/or emission can be important is indicated by the optical properties of the medium; the best indicators are the mass extinction coefficient (α) which influences total extinction, the single scattering albedo ($\tilde{\omega}_0$) which indicates the fractional amount of scattering, and $1 - \tilde{\omega}_0$ which indicates the fractional amount of absorption.

²R. A. Sutherland et al, 1979, "A Real Time Satellite Data Acquisition, Analysis and Display System-A Practical Application of the GOES Network," J Appl Meteorol, 3:355-360

³E. Chen et al, 1979, "Satellite-Sensed Winter Nocturnal Temperature Patterns of the Everglades Agricultural Area," J Appl Meteorol, 8:992-1002

⁴C. D. Kern, 1965, "Evaluation of Infrared Emission of Clouds and Ground as Measured by Weather Satellites," Environmental Research Papers, No. 155, AFCRL-65-840, Air Force Cambridge Research Laboratories, Hanscom Air Force Base, MA

⁵S. M. Greenfield and W. W. Kellogg, 1960, "Calculations of Atmospheric Infrared Radiation as seen from a Meteorological Satellite," J Meteorol, 6:283-290

Inventory smokes have $\tilde{\omega}_0 \approx 1$ in the visible,⁶ indicating a predominance of scattering, and $\tilde{\omega}_0 \approx 0$ in the infrared, indicating a predominance of absorption, and consequently emission. Thus path radiance is important and perhaps even of overriding significance for inventory smokes from the visible through the infrared.

The need for further model development in this area was established in an earlier study¹ which made a detailed examination of the Army inventory of existing smoke and dust obscuration models. A major finding of this work was that although most models reported capabilities for treating attenuation, all were deficient in wholly treating path radiance for wavelengths through the infrared.

As a step toward filling this technological gap, an improved smoke obscuration model reported herein was developed. Since three of the models studied (SOM II,⁷ HECSOM,⁸ and ACT-I,⁹ did report some capabilities in the visible, the most promising, ACT-I,* was chosen as a starting point (hence the acronym ACT-II for the present model).

The approach is to provide optical information critical to the needs of presently existing electro-optical system performance and smoke effectiveness models. An informal survey disclosed that the requirements were reducible to the following fundamental quantities:

1. Ambient irradiance (light level),
2. Target and background radiance,

⁶R. C. Shirkey and R. A. Sutherland, 1981, "Aerosol Phase Function Data Base," chapter 16, EOSAEL 80, Volume I, Technical Documentation, editor L. D. Duncan, ASL-TR-0072, US Army Atmospheric Sciences Laboratory, White Sands Missile Range, NM (AD B055130L)

¹R. A. Sutherland, D. W. Hoock, and R. B. Gomez, 1981, An Objective Summary of US Army Electro-Optical Modeling and Field Testing in an Obscurant Environment, ASL-TR-0096, US Army Atmospheric Sciences Laboratory, White Sands Missile Range, NM

⁷Smoke Obscuration Model II (SOM II) Computer Code Volume II - Analyst Manual, 1979, JTCG/ME Smoke and Aerosol Working Group Document 61, JTCG/ME-78-9-2

⁸R. K. Dumbauld and H. Bjorklund, 1977, Mixing Layer Analysis Routine and Transport/Diffusion Application Routine for EPAMS, ECOM-77-2, Atmospheric Sciences Laboratory, US Army Electronics Command, White Sands Missile Range, NM

⁹R. B. Gomez, R. Pennsyle, and D. Stadlander, 1979, "Battlefield Obscuration Model, ACT I," Proceedings of Smoke Symposium III, Harry Diamond Laboratories, Adelphi, MD

*The acronym ACT derives from the developing agencies Atmospheric Sciences Laboratory, Chemical Systems Laboratory, and TRASANA.

3. Line of sight (LOS) transmission, and

4. LOS path radiance,

where target and background radiances are computed for both the unperturbed (smoke free) and smoked environment, and LOS data are provided for both the observer-target and observer-background. From these fundamental quantities other specialized data such as contrast or apparent resolvable temperature can be determined easily for input to existing system performance and smoke effectiveness models such as the target acquisition model of the Night Vision and Electro-Optics Laboratory¹⁰ or the munition expenditures models described by Pennsyle¹¹ and Hoock.¹²

In another respect care is taken so that the (present) model inputs are compatible with the outputs of other associated models such as LOWTRAN¹³ and AGAUS¹⁴ as well as with data collected during field tests such as Smoke Week II.¹⁵

Although the primary focus is on optical phenomena, the important aspect of obscurant transport and diffusion has not been ignored. The approach here is to generalize procedures so that the model will accommodate any arbitrary ensemble of Gaussian smoke clouds, providing a convenient framework for possible future union with equivalent generalized transport and diffusion models. Most present models, however, do not provide cloud temperature which is critical for the infrared. Thus a Gaussian diffusion model was developed based

¹⁰"Combat Simulation Target Acquisition Model and Data Input" (U), CONFIDENTIAL, 1980, Draft Technical Report, US Army Night Vision and Electro-Optics Laboratory, Fort Belvoir, VA (in process)

¹¹R. O. Pennsyle, 1979, Methodology for Estimating Smoke/Obscurant Munition Expenditure Requirements, ARCSL-TR-79022, Chemical Systems Laboratory, Aberdeen Proving Ground, MD

¹²D. W. Hoock, 1981, "SCREEN," chapter 5, EDSAEL 80, Volume 1, Technical Documentation, editor L. D. Duncan, ASL-TR-0072, US Army Atmospheric Sciences Laboratory, White Sands Missile Range, NM (AD B055130L)

¹³J. E. Selby et al, 1978, "Atmospheric Transmittance/Radiance: Computer Code LOWTRAN 4," Environmental Research Papers, No. 626, AFGL-TR-78-0053, Air Force Geophysics Laboratory, Hanscom Air Force Base, MA

¹⁴R. C. Shirkey et al, 1980, Single Scattering Code AGAUSX: Theory, Applications, Comparisons, and Listing, ASL-TR-0062, US Army Atmospheric Sciences Laboratory, White Sands Missile Range, NM

¹⁵DPG Final Test Report on Smoke Week II at Eglin AFB, FL (U), CONFIDENTIAL, 1978, Volumes I and II, DPG-FR-78-317, Dugway Proving Ground, UT

upon commonly used procedures^{16 17} and extended to include buoyant rise and cloud temperature using fundamental principles.^{18 19}

The work is divided into three parts: the present work covers theory and examples, a second²⁰ covers program documentation and a users guide, and a third²¹ covers validation and applications.

Historically the problem of path radiance and its significance to visible perception have been recognized by the Army modeling community for several years. As early as 1972 an unpublished document described a smoke obscuration model (SOM) which reported to compute visible contrast and was later accepted as the Joint Technical Coordinating Group (JTCG) working model. This early model was expanded by at least two groups, one leading to the development of the model SOM II⁷ and another to ASLSOM which was further modified to become the ACT model⁹ which is the direct forerunner of the present model.

2. OUTLINE AND SCOPE

The fundamental optical quantities to be determined in addition to transmission are the amounts of radiant energy received by an observer from the two directions (approximately coincident) defined by the relative positions of a

¹⁶Smoke Effectiveness Manual, 1979, JTCG/ME Smoke and Aerosol Working Group Document Number FM 101-61-8

¹⁷F. V. Hansen, 1979, Engineering Estimates for the Calculation of Atmospheric Dispersion Coefficients, ASL Internal Report, US Army Atmospheric Sciences Laboratory, White Sands Missile Range, NM

¹⁸F. Pasquill, 1974, Atmospheric Diffusion, second edition, Halsted Press Div., John Wiley and Sons, Inc., New York

¹⁹C. H. B. Priestley, 1956, "A Working Theory of the Bent-Over Plume of Hot Gas," Quart J Roy Meteorol Soc, 82:165-176

²⁰R. A. Sutherland and D. Clayton, 1981, An Improved Smoke Obscuration Model Act II: Part 2 Documentation and User Guide, Technical Report, US Army Atmospheric Sciences Laboratory, White Sands Missile Range, NM (in process)

²¹R. A. Sutherland, 1981, "Comparisons Between the Improved Smoke Obscuration Model ACT II and Recent Smoke Week Data," Proceedings of Smoke Symposium V, Harry Diamond Laboratories, Adelphi, MD

⁷Smoke Obscuration Model II (SOM II) Computer Code Volume II - Analyst Manual, 1979, JTCG/ME Smoke and Aerosol Working Group Document 61, JTCG/ME-78-9-2

⁹R. B. Gomez, R. Pennsyle, and D. Stadlander, 1979, "Battlefield Obscuration Model, ACT I," Proceedings of Smoke Symposium III, Harry Diamond Laboratories, Adelphi, MD

target and background, both treated as Lambertian surfaces. The radiance incident at the observer from each direction is generally composed of two parts: (1) the direct radiance emitted and reflected by the target (or background) then transmitted (with some loss due to extinction) along the LOS to the observer and (2) the diffuse, or path, radiance emitted and scattered by suspended material (smoke) at all points (such as P in figure 2) along the LOS then transmitted (again with some loss due to extinction) a remaining distance to the observer, giving rise to a path radiance. One aspect of the problem which causes major complexity is that the entire environmental sphere must be considered the source for the reflected and diffuse radiation, thus requiring integration over all angles, not only at the target and background but also at all points along the LOS. Except for rare circumstances, these integrations must be carried out by some approximate numerical technique. The approach taken here is to divide the sky hemisphere into discrete angular sectors and then assume that the radiances from the various sectors are either known from measurement (as in recent field tests) or produced by some appropriate model (perhaps LOWTRAN¹³). Terrain radiance due to reflected sky radiation and thermal emission can then be calculated from knowledge of surface albedo, emissivity, and temperature to complete the characterization of the (smoke free) radiation environment, which is then assumed constant throughout. The exact sectoring procedure used in the model is outlined in section 3.

Mathematically the problem can be summarized by the following formal expression describing radiant propagation along a straight path over a distance r .²²

$$R(\vec{r}) = R(\vec{r}_0) e^{-\tau(\vec{r}, \vec{r}_0)} + \int_{\vec{r}_0}^{\vec{r}} [J(\vec{r}', \theta, \phi) + (1 - \tilde{\omega}_0)B(\lambda, T_p)] e^{-\tau(\vec{r}, \vec{r}')} \frac{d\tau}{dr} d\vec{r}' \quad (4)$$

where $R(\vec{r})$ is the radiance incident at \vec{r} ; $R(\vec{r}_0)$ is the radiance of the target (or background) located at \vec{r}_0 ; and θ, ϕ are the polar angles defining the path of propagation (that is, the LOS). Although the vector notation will be dropped, it is assumed here and in the following that the observer is at the origin and that the coordinates are rotated so that \vec{r} and \vec{r}' lie along the LOS (figure 4). Generally the term $J(r, \theta, \phi)$ (called the source function) accounts for scattering into the LOS, and $(1 - \tilde{\omega}_0)B(\lambda, T_p)$ accounts for emission from increments along the LOS.

¹³J. E. Selby et al, 1978, "Atmospheric Transmittance/Radiance: Computer Code LOWTRAN 4," Environmental Research Papers, No. 626, AFGL-TR-78-0053, Air Force Geophysics Laboratory, Hanscom Air Force Base, MA

²²S. Chandrasekhar, 1960, Radiative Transfer, second edition, Dover Press Publications, Inc., New York

The Planck or blackbody function of equation (4) is written explicitly as

$$B(\lambda, T_p) = \frac{2hc^2\lambda^{-5} \Delta\lambda}{[\exp(hc/kT_p) - 1]} \quad (5)$$

where λ is the wavelength, $\Delta\lambda$ the bandpass, and h , k , and c are, respectively, the Planck constant, the Boltzmann constant, and the speed of light in vacuum. The obscurant temperature (T_p) is assumed variable over the path, so that B contains an implicit dependence on r .

The optical thickness (τ) is defined as

$$\tau(r, r') = \int_{r'}^r \alpha C(r'') dr'' , \quad (6)$$

where α is the obscurant mass extinction coefficient and C is the obscurant concentration. Both obscurant temperature and concentration are discussed in section 5.

The source function $J(r, \theta, \phi)$ is difficult to compute, requiring integrations over the entire environmental sphere accounting for the angular characteristics of both the ambient radiation and the scattering medium. Except for trivial cases, no exact methods exist for computing this term; and for realistic scenarios, some approximate technique must be employed. The model uses the single scattering approximation in which the source function can be written as

$$J(r, \theta, \phi) = \frac{1}{4\pi} \int_{4\pi} P(\theta_s) L(\theta', \phi') e^{-\tau(r, r_s)} d\Omega' , \quad (7)$$

where θ_s is the scattering angle (figure 2) and P the phase function. The term $L(\theta', \phi')$ consists of two parts: the source radiance $R_s(\theta', \phi')$ from the directions of the sky and terrain sectors and the thermal emission along these same directions. Mathematically,

$$L(\theta', \phi') = R_s(\theta', \phi') + (1 - \tilde{\omega}_0) \int_r^{r_s} B(\lambda, T_p) e^{[\tau(r, r_s) - \tau(r, r')]} dr' . \quad (8)$$

In the above expressions, r is distance to any point along the LOS; r' is distance from that point along the direction defined by θ' , ϕ' ; r_s is distance to the sky and terrain sources; and $d\Omega'$ is the differential solid angle.

For inventory smokes (and neglecting polarization), the angular dependence of the phase function is dependent only upon the scattering angle, which from simple geometry is given by (see figure 2):

$$\cos \theta_s = [\cos \theta \cos \theta' + \sin \theta \sin \theta' \cos(\phi - \phi')] . \quad (9)$$

Some caution is required in using equation (9) to assure the proper algebraic sign. For use in the phase function equation (9) is correct as it stands, but for Lambertian surfaces (that is, target, background, etc.) the sign must be reversed because the convention used in the model requires the surface normal pointing positive inward (for example, away from the observer) which in turn requires the reversal in sign.

The phase function is required as input but can readily be obtained from the associated model AGAUS,¹⁴ one version of which is distributed with the Electro-Optical Systems Atmospheric Effects Library (EOSAEL 80²³). The phase function is assumed to be normalized such that

$$\frac{1}{4\pi} \int_{4\pi} P(\theta_s) d\Omega = \tilde{\omega}_0 , \quad (10)$$

but in the model it is renormalized via equation (10) to a single scattering albedo specified as input. However, to be strictly compatible with theory the input single scattering albedo should be that computed from Mie scattering.

The major objective of the model is to evaluate the two components of equation (4), once for the observer-target and once for the observer-background by using the procedures described by equations (4) through (9). For the special case of computing $R(r_0)$, the target or background radiance, the same procedure for the second term of equation (4) is used except that the factor $\frac{1}{4\pi} P(\theta_s)$ in equation (7) is replaced by $(a \cos \theta_s / \pi)$ which assumes a Lambertian surface of albedo* (a) with surface normal along the LOS. Also for these cases the computations are restricted to $\theta_s > 90^\circ$ to avoid contributions due to reflection from the rear surface. The (smoke free) surface irradiance (E_{sfc}) is also computed in the same manner with $\theta = \phi = 0$ (vertical) and the factor $1/\pi$

¹⁴R. C. Shirkey et al, 1980, Single Scattering Code AGAUSX: Theory, Applications, Comparisons, and Listing, ASL-TR-0062, US Army Atmospheric Sciences Laboratory, White Sands Missile Range, NM

²³R. A. Sutherland, 1981, "Smoke Obscuration Model," chapter 3, EOSAEL 80, Volume 1, Technical Documentation, editor L. D. Duncan, ASL-TR-0072, US Army Atmospheric Sciences Laboratory, White Sands Missile Range, NM (AD B055130L)

*For opaque surfaces, reflectivity (r), albedo (a), and emissivity (ε) are related as (a = r and ε = 1 - r).

removed. In all cases, an emission term of the form $\epsilon B(\lambda, T)$ is added where T is chosen appropriately as the surface, target, or background temperature, and the emissivity (ϵ) is computed from the reflectivity or albedo as $\epsilon = (1 - a)$. The (smoke free) surface irradiance is used later (see equation (18)) to compute radiances for terrain sectors which are then treated in the same manner as sky sectors.

For the visible scenarios, the effect of emission will be negligible because of the smallness of the blackbody function in these spectral regions at nominal temperatures. For infrared scenarios, this term often dominates, being more pronounced at higher temperature, which means that errors due to neglect of multiple scattering will be minimal in the infrared. However, errors may occur in the infrared due to uncertainties in the cloud temperature.

The process to be modeled here can be summarized in geometrical terms with the aid of figure 2. Simply stated, the problem is to compute contributions to path radiance at each point P along the LOS, and then to sum over all such points. At each increment, effects of extinction must be included over the remaining path \overline{PO} to the observer. At each point P the contribution is composed of two parts--one due to scattering into the increment from all angles and the other due to emission by the increment. The single scattering approximation assumes that the radiance along any path \overline{SP} is scattered into the LOS only once and that this scattering occurs at P . Thus the radiance scattered into the LOS at point P consists of the source radiance, R_s , reduced by extinction over the path \overline{SP} , plus the summation of the emission from each element P' along the path \overline{SP} ; the emissive contribution of each element is reduced by extinction over the path $\overline{PP'}$. The total scattering contribution of each increment at P is found by summing over all angles, accounting for angular scattering properties of the medium via the phase function. Total path radiance is found by summing over all increments along \overline{OT} .

In the model the increment spacings are chosen by a criterion based upon the incremental optical depth $\Delta\tau$. This method speeds computations by avoiding insignificant contributions for increments containing no obscurant which would occur for a criterion based on spatial separation (Δr). The minimum spacing in the model however is normally defaulted to 1 m.

The model treats extinction due to the ambient atmosphere by appropriately modifying transmission (i.e., $T_{LOS} = T_{smoke} T_{atmos}$) for propagation along the LOS. This option is employed by way of a user supplied volume extinction coefficient, (σ), so that $T_{atmos} = e^{-\sigma L}$, where L is distance of propagation. Parallel point sources of radiation, including the sun or moon, are also treated by the model.

In all of the above computations, the model computes optical thickness (τ) by assuming the medium composed of any ensemble of obscuring smoke clouds defined by centroid locations, Gaussian standard deviations, and temperature. Methods for integrating equation (6) and for producing the ensemble are given in later sections of the report.

3. AMBIENT IRRADIANCE (SECTORING SCHEME)

This section describes the sectoring scheme used to simulate incoming radiation from sky and terrain which will then be used to approximate terms for the source function of equation (8). Throughout this section repeated use will be made of approximations, assuming that scenario relative distances are small in comparison to spatial variations in ambient conditions. This process considerably simplifies the geometry by allowing all scenario elements to be treated as exposed to the same ambient radiational environment. These are approximations often used in problems of this type and introduce only minimal errors.

The major divisions of the entire 4π steradians comprising the environmental sphere are sketched in figure 3. The upper sector is assumed to be comprised of sky (including sun, moon, and clouds) and the lower to be overall flat terrain. Both sky and terrain will be treated as sources of ambient radiation, the latter through reflection of sky radiation and thermal emission.

To facilitate computations, the two major regimes are further subdivided into angular sectors subtending equal solid angles. These discrete sectors are then treated as point sources of parallel radiation emanating from the direction of the sector midpoint. Additional sources of radiation such as the sun or moon are superimposed at their appropriate angular positions. The model will accommodate variable radiance from each of the discrete sky sectors, but to maintain consistency with the assumptions mentioned earlier, one must assume that the terrain is homogeneous in albedo, emissivity, and temperature.

The procedure for sectoring the two regimes into equal angular sectors follows directly from the definition of solid angle; $d\Omega_{\theta, \phi} = \sin \theta \, d\theta \, d\phi$, where θ and ϕ are the usual zenith and azimuth angles.

The azimuthal sectoring is particularly simple since integration over contiguous divisions (ϕ_i, ϕ_{i+1}) yields, simply, $d\Omega_{\theta} = \Delta\phi \sin \theta \, d\theta$, where $\Delta\phi = \phi_{i+1} - \phi_i$ is the azimuthal separation, which for m sectors is simply $\Delta\phi = 2\pi/m$. The representative midpoints are then

$$\phi_i = (i - 1)\pi/m . \quad (11)$$

For the zenith sectors, the integration between contiguous divisions yields

$$\Delta\Omega = \Delta\phi(\cos \theta_j - \cos \theta_{j+1}) . \quad (12)$$

For n sectors, all of which are equal and contained in a total solid angle 2π , we have

$$\Delta\phi(\cos \theta_j - \cos \theta_{j+1}) = 2\pi/nm , \quad (13)$$

which after substituting for $\Delta\phi$ and rearranging becomes

$$\cos \theta_{j+1} = \cos \theta_j - 1/n , \quad (14)$$

from which all divisions can be calculated by knowing that $\theta_1 = 0$. An equivalent but sometimes more convenient expression is

$$\cos \theta_j = 1 - (j - 1)/n . \quad (15)$$

Further reasoning yields the following equation for sector midpoints:

$$\cos \bar{\theta}_j = 1 - (2j - 1)/2n . \quad (16)$$

The corresponding distances to the terrain sector midpoints are

$$r_s^{j,j} = h/\cos \bar{\theta}_j , \quad (17)$$

where h is the vertical distance from the surface for the particular scenario element under consideration. The radiance from the sector, assuming a Lambertian surface is

$$R = [(a/\pi)E_{sfc} + (1 - a)B(\lambda, T_{sfc})] , \quad (18)$$

where a , E_{sfc} , and T_{sfc} are, respectively, the surface albedo, irradiance (see section 2), and temperature. From this point on, the only difference in treating sky or terrain sectors is that the finite distance to the terrain sectors must be considered via equation (17), whereas the sky sectors can be assumed at infinity (actually 10,000 m in the model).

Ordinarily one does not have sufficient data, or the inclination, to provide the radiance values for all of the sectors used in the model; therefore, the model was programmed to proportion the sectors uniformly by interpolating the input radiance values from arbitrary angles. This interpolation makes the model input directly compatible with sky radiance data from the smoke tests.

Also, to avoid inconsistencies between the computed surface irradiance (E_{sfc}) and the reported measurements,²¹ the sun and sky input data are treated only as relative and are normalized so as to reproduce the measured value when integrated over the sky hemisphere. Thus the model as now coded requires only relative data from sun and sky but an absolute determination of surface irradiance. In effect this method reduces the complexity of the required input.

4. OPTICAL THICKNESS CALCULATIONS

This section describes the general method used to compute smoke concentration $C(r)$ and optical thickness. Throughout we will assume a constant extinction coefficient so that the optical depth is simply the product (αCL) where CL is the line integrated concentration, commonly called CL product.

The methodology is based upon the general assumption that a smoke plume or cluster can be represented by a series of spatially and temporally discrete overlapping clouds each with concentration given by a trivariant Gaussian function. This is a common assumption used in many models although the manner of spacing and sizing such clouds may vary from model to model. For this latter reason the methodology is kept general so as to be easily adaptable to various cloud transport models.

For some i^{th} cloud centered at \bar{X}_i , \bar{Y}_i , and \bar{Z}_i the concentration (due to this source only) is given by

$$C_i(x, y, z) = (2\pi)^{-3/2} \frac{Q_i}{\sigma_x^i \sigma_y^i \sigma_z^i} e^{-1/2 \left[\left(\frac{x - \bar{X}_i}{\sigma_x^i} \right)^2 + \left(\frac{y - \bar{Y}_i}{\sigma_y^i} \right)^2 + \left(\frac{z - \bar{Z}_i}{\sigma_z^i} \right)^2 \right]} \quad (19)$$

where Q_i is the total mass of the cloud and accounts for (1) munition fill mass expended during the burn producing the cloud, (2) munition efficiency, and (3) smoke yield factor. The total concentration is found by summing the concentrations of all such clouds.

²¹R. A. Sutherland, 1981, "Comparisons Between the Improved Smoke Obscuration Model ACT II and Recent Smoke Week Data," Proceedings of Smoke Symposium V, Harry Diamond Laboratories, Adelphi, MD

It is convenient to rewrite equation (19) in spherical coordinates to give an expression for concentration along an LOS defined as before by polar angles θ and ϕ at some arbitrary point a distance r from the origin. It is straightforward to show that the equivalent to equation (19) is

$$C(r, \theta, \phi) = \frac{(2\pi)^{-3/2} Q}{\sigma_x \sigma_y \sigma_z} e^{-1/2 \left[\left(\frac{\alpha r - x_0}{\sigma_x} \right)^2 + \left(\frac{\beta r - y_0}{\sigma_y} \right)^2 + \left(\frac{\gamma r - z_0}{\sigma_z} \right)^2 \right]} \quad (20)$$

where the indices have been dropped to avoid cumbersome notation. The line parameters α , β , γ and offsets x_0 , y_0 , z_0 are:

$$\begin{aligned} \alpha &= \sin \theta \sin \phi & x_0 &= \bar{X}_i - x_1 \\ \beta &= \sin \theta \cos \phi & y_0 &= \bar{Y}_i - y_1 \\ r &= \cos \theta & z_0 &= \bar{Z}_i - z_1 \end{aligned} \quad (21)$$

where x_1 , y_1 , and z_1 are coordinates of any point on the LOS, taken in the model to be the common point such as P in figure 4.

With considerably more algebraic manipulation which involves expanding the expression in the exponential, rearranging and then rewriting the resultant expression as a perfect square, the following expression results:

$$C_i(r, \theta, \phi) = Q_i' e^{-1/2 \left(\frac{r - \bar{R}_i}{\Sigma_i} \right)^2} \quad (22)$$

which is itself a Gaussian with mean \bar{R}_i , standard deviation Σ_i , and strength Q_i' given by the following expressions, again with indices suppressed:

$$\begin{aligned} \bar{R} &= \frac{\alpha x_0 (\sigma_z \sigma_y)^2 + \beta y_0 (\sigma_x \sigma_z)^2 + \gamma z_0 (\sigma_x \sigma_y)^2}{(\alpha \sigma_y \sigma_z)^2 + (\beta \sigma_x \sigma_z)^2 + (\gamma \sigma_x \sigma_y)^2} \\ \Sigma &= \frac{\sigma_x \sigma_y \sigma_z}{[(\alpha \sigma_y \sigma_z)^2 + (\beta \sigma_x \sigma_z)^2 + (\gamma \sigma_x \sigma_y)^2]^{1/2}} \end{aligned} \quad (23)$$

$$Q' = \frac{(2\pi)^{-3/2} Q}{\sigma_x \sigma_y \sigma_z} e^{-1/2} \left[R_\sigma - \left(\frac{R}{\Sigma} \right)^2 \right]$$

$$R_\sigma = \left(\frac{x_0}{\sigma_x} \right)^2 + \left(\frac{y_0}{\sigma_y} \right)^2 + \left(\frac{z_0}{\sigma_z} \right)^2$$

(23) cont

The final desired result for line integrated concentration beginning at point $P(x_1, y_1, z_1)$ along the line described by (α, β, γ) for a distance D becomes (see figure 4):

$$CL_i(D, \theta, \phi)\sqrt{\pi}/2 = Q'_i \Sigma_i \left[\operatorname{erf} \left(\frac{D - R_i}{\sqrt{2\Sigma_i}} \right) + \operatorname{erf} \left(\frac{R_i}{\sqrt{2\Sigma_i}} \right) \right] \quad (24)$$

where the error function is defined as

$$\operatorname{erf}(x) = \frac{2}{\sqrt{\pi}} \int_0^x \exp(-t^2) dt \quad (25)$$

and is computed in the model according to the approximate technique as described by Abramowitz and Stegun.²⁴

The formulation here applies in a wind vector aligned coordinate system requiring that scenario Cartesian coordinates and angles be transformed to this system before the calculations.

The model assumes both concentration and temperature to be Gaussian so that a relationship analogous to equation (24) is used to obtain temperature of various line segments for computation of thermal emission. Also symmetric "image" clouds accounting for surface particulate reflection are included in the usual manner.²³

5. CLOUD CONCENTRATION AND TEMPERATURE

The preceding sections assumed a transport and diffusion model generating some pattern of overlapping Gaussian clouds. Several methodologies which can be

²⁴M. Abramowitz and I. Stegun, 1970, Handbook of Mathematical Functions, Dover Press Publications, Inc., New York

²³R. A. Sutherland, 1981, "Smoke Obscuration Model," chapter 3, EOSAEL 80, Volume 1, Technical Documentation, editor L. D. Duncan, ASL-TR-0072, US Army Atmospheric Sciences Laboratory, White Sands Missile Range, NM (AD B05513JL)

adapted to this general concept are available. We borrow bits and pieces from these methodologies to produce a submodel to be used for the validation studies reported later. Production of this model consists of generating the parameters Q_i , $(\bar{X}_i, \bar{Y}_i, \bar{Z}_i)$, $(\sigma_x^i, \sigma_y^i, \sigma_z^i)$, and cloud temperature which will now be covered in order.

5.1 Smoke Source Function (Q)

The factor Q represents the total mass of a smoke cloud and is composed of the product of factors M, λ , and Y where M is the mass of munition fill expended during the burn producing the cloud, λ is the chemical efficiency with which the mass is converted to actual smoke nuclei, and Y is the smoke yield factor which accounts for increased mass due to hygroscopic interactions with the ambient air mass.

For instantaneous bursts such as bulk fill white phosphorus munitions, a single cloud of mass $Q = M \lambda Y$ is used. For munitions of extended burning time (> 1 s), the plume is generated as a series of discrete puffs produced during short time increments (nominally 1 s). Variable burn rate is included by employing either a quadratic or exponential function with coefficients as determined empirically from field tests. The EOSAEL 80 Technical Documentation²³ contains a review of these burn coefficients and other munition characteristics.

5.2 Cloud Centroids (\bar{X} , \bar{Y} , and \bar{Z})

With the coordinate system rotated to align the positive x axis along the wind vector and assuming the cloud to be transported by the mean wind (\bar{U}), the cloud centroids are modeled as

$$\begin{aligned}\bar{X} &= \bar{U} + X_m \\ \bar{Y} &= Y_m \\ \bar{Z} &= Z_m + H(t)\end{aligned}\tag{26}$$

where X_m , Y_m , and Z_m are munition coordinates. The method of computing the cloud rise function $H(t)$ which also involves the cloud temperature is discussed later. The mean windspeed is computed by averaging vertically over the

²³R. A. Sutherland, 1980, "Smoke Obscuration Model," chapter 3, EOSAEL 80, Volume 1, Technical Documentation, editor L. D. Duncan, ASL-TR-0072, US Army Atmospheric Sciences Laboratory, White Sands Missile Range, NM (AD B055130L)

significant cloud extent (3σ) using the usual windspeed power law: $U(z) = U_r(z/z_r)^P$ where U_r is the windspeed at an (input) reference height (Z_r) and P is the vertical profile exponent.

5.3 Dispersion Functions ($\sigma_x, \sigma_y, \sigma_z$)

The dispersion functions $\sigma_x, \sigma_y, \sigma_z$ are all expressed as power functions of the x centroid with initial offset, $\sigma(0)$; that is,

$$\sigma_{x, y, z} = \sigma(0) + \left(\frac{X - C}{A} \right)^B \quad (X \text{ in meters}) \quad (27)$$

The source sigmas $\sigma(0)$, essentially representing the dimensions of the cloud at $t = 0$ are modeled by the following power functions which were derived from the data of AMSAA TR-201.²⁵

$$\begin{aligned} \sigma_{x, y}(0) &= 5.0 Q^{0.3} \\ \sigma_z(0) &= 1.7 Q^{0.3} \end{aligned} \quad (Q \text{ in kilograms}) \quad (28)$$

The diffusion parameters A and B of equation (27) are modeled as functions of the surface average roughness element (Z_0) and the stability category as listed in table 1. For surface roughness $Z_0 > 0$, the values are those cited by Hansen;¹⁷ and for these cases the parameter C of equation (27) is set to zero. For a roughness entered as $Z_0 < 0$ (default), the method of the Smoke Effectiveness Manual¹⁶ is used, in which case the initial sigmas are absorbed in the parameter C , and the term $\sigma(0)$ is set to zero.

²⁵Analysis of the Smoke Cloud Data from the August 1975 Jefferson Proving Ground Smoke Test, 1977, AMSAA Technical Report TR-201, Aberdeen Proving Ground, MD (AD A045874)

¹⁷F. V. Hansen, 1979, Engineering Estimates for the Calculation of Atmospheric Dispersion Coefficients, ASL Internal Report, US Army Atmospheric Sciences Laboratory, White Sands Missile Range, NM

¹⁶Smoke Effectiveness Manual, 1979, JTCG/ME Smoke and Aerosol Working Group Document Number FM 101-61-8

Following the methodology cited by Hansen,¹⁷ σ_x , σ_y , and σ_z are reduced by factors 0.74, 0.67, and 0.67, respectively, for instantaneous sources.

5.4 Cloud Temperature and Buoyant Rise

Current methods for modeling buoyant rise are generally limited to empirical methods based upon observations of factory smoke stack effluents²⁶ or curve fits to data from field tests.²⁵ These procedures, although of approximate validity for special circumstances, have severe shortcomings for the general case where it becomes necessary to simultaneously model cloud temperature consistently. This consistency is particularly important in the infrared where cloud temperature acquires an added significance of its own in addition to the indirect effect on buoyancy. The method developed for the model applies basic principles and certain simplifying assumptions borrowing heavily from earlier works^{18 19} in a self-consistent numerical scheme as outlined below.

The buoyant motion is modeled by treating each cloud of the ensemble as though independent of other clouds, an assumption consistent with the transport and diffusion methodology discussed earlier. Initial cloud temperature is modeled by equating the internal thermal energy of each instantaneous cloud to the energy expended during the exothermal reaction producing the cloud. Assuming, as before, similar distributions in both temperature and concentration, the following expression results for initial cloud temperature:

$$T_c = \frac{E C_o + \rho C_p T_z}{\rho C_p}, \quad (29)$$

where E is the obscurant heat of reaction (calorie/gram), C_o the mean concentration, ρC_p the volumetric specific heat of the ambient air ($290 \text{ cal m}^{-3} \text{ }^\circ\text{C}^{-1}$), and T_z the ambient air temperature at the cloud centroid. The use of equation (29) assumes complete thermal mixing between cloud and entrained air.

²⁶G. A. Briggs, 1965, "A Plume Rise Model Compared with Observations," J Air Poll Control Assoc, 15:433

²⁵Analysis of the Smoke Cloud Data from the August 1975 Jefferson Proving Ground Smoke Test, 1977, AMSAA Technical Report TR-201, Aberdeen Proving Ground, MD (AD A045874)

¹⁸F. Pasquill, 1974, Atmospheric Diffusion, second edition, Halsted Press Div., John Wiley and Sons, Inc., New York

¹⁹C. H. B. Priestley, 1956, "A Working Theory of the Bent-Over Plume of Hot Gas," Quart J Roy Meteorol Soc, 82:165-176

The vertical (ambient) temperature profile is modeled as

$$T_z = T_r + T_0 \frac{1 - \exp[-\alpha(z - z_r)/H_m]}{1 - \exp[-\alpha(H_m - z_r)/H_m]} \quad z \leq H_m/10$$

$$T_z = T_{10} + \left[\frac{T_{hm} - T_{10}}{H_m - H_m/10} \right] z \quad z > H_m/10 \quad (30)$$

$$T_{10} = T_z(H_m/10) ,$$

where T_r is the temperature measured at the reference height (z_r), T_{hm} is the temperature at the mixing height (H_m), and α is chosen so as to fit to the measured ambient temperature gradient at the reference height and to the adiabatic lapse rate (0.00966°C/m) at $z = H_m/10$.

The vertical velocity (ω) at any later time is found by first applying the conservation of momentum along the vertical:

$$\frac{d\omega}{dt} = \frac{g}{T_z} \Delta T - k_m \omega , \quad (31)$$

where ΔT is cloud temperature excess, g is the acceleration due to gravity, T_z as before is the (absolute) ambient air temperature at the centroid height, and k_m is the momentum mixing coefficient taken to be 0.10 s^{-1} .¹⁹

Equation (31) with (29) and (30) is then solved for ω using reiterative techniques assuming zero initial velocity to further determine the rise function by way of the following kinematic relations:

$$\omega(t) = \omega(t - \Delta t) + (d\omega/dt)\Delta t;$$

$$H(t) = H(t - \Delta t) + \omega(t)\Delta t . \quad (32)$$

¹⁹C. H. B. Priestley, 1956, "A Working Theory of the Bent-Over Plume of Hot Gas," Quart J Roy Meteorol Soc, 82:165-176

The process is then repeated by incrementing time (and hence C) over the "age" of the cloud. Beyond the first time increment, a term $[(\Delta T) \times \Delta C/C]$ is sequentially added to equation (29) to account for the vertically changing temperature of the ambient entrained air. In actual practice the time increment is computed so as to limit the cloud rise increment to 1 m or less to assure convergence of the numerical procedure.

6. EXAMPLE (FROM SMOKE WEEK II)

6.1 Conversion of Model Results

As mentioned in section 1, the model was coded in such a way as to be compatible with measurements made during the major field tests. This coding allows nearly direct comparison between model results and measured data. However, a word of caution is required to interpret the results appropriately.

The model has assumed radiometric units throughout, whereas the units reported in the field tests are mixed; that is, sky and solar data are in radiometric units, but target, background, and path radiance are in photopic units. Because the underlying spectrum is not uniform (that is, the sky is blue, clouds are white, and the sun is yellow-green), some error and confusion result when converting between the two systems. Rather than try to correct for the nonuniform spectrum (a procedure which could only increase the error), we choose here to assume the spectrum nearly uniform and convert the model results to photopic units by using the standard photopic response curve²⁷ which can be closely approximated by the following Gaussian function (see figure 5):

$$R_p = R_0 \exp[-1/2(\lambda - \lambda_0)/\sigma]^2], \quad (33)$$

where

$$R_0 = 673 \text{ lm/W},$$

$$\lambda_0 = 0.56 \mu\text{m},$$

$$\sigma = 0.0426 \mu\text{m},$$

²⁷A. Stimson, 1974, Photometry and Radiometry for Engineers, John Wiley and Sons, Inc., New York

which can be integrated to yield the following conversion factor:

$$E(lm) = R_0 \sqrt{2\pi} \sigma E(W) , \quad (34)$$

or in terms of bandwidth (full width at half maximum):

$$E(lm) = R_0 \left[\frac{\pi}{2 \ln 2} \right]^{1/2} \Delta\lambda E(W) . \quad (35)$$

Both the bandwidth ($\Delta\lambda$) and position of maximum response (λ_0) are input by the user and are $0.100\mu\text{m}$ and $0.56\mu\text{m}$ for straight photopic conversion. For input wavelengths other than $0.56\mu\text{m}$, the model shifts and reduces the peak response via a multiplicative Gaussian factor:

$$f = \exp \left[-1/2 \left(\frac{\lambda_i - 0.56}{\sigma} \right)^2 \right] \quad (36)$$

which is equal to unity for $\lambda = 0.56$ and is essentially zero for the infrared. In all cases the model also provides output in radiometric units.

Also the Smoke Week sun and sky radiances are reported for a detector field of view of 1° requiring division by $(\pi/180)^2$ to convert to a unit steradian. This conversion is not required for the input to the model as now coded since these data are used only in a relative sense. For sake of completeness, some further required conversion factors are:

1 footcandle = 10.76 lumens per square meter

$$1 \text{ footlambert} = \frac{10.76}{\pi} \text{ candles per square meter} \quad (37)$$

1 candle = 1 lumen per steradian

6.2 Input Data

Trial 1 of the Smoke Week II field test, held at Eglin Air Force Base, Florida, in November 1978 consisted of the detonation of 15 155-mm hexachloroethane (HC) Type M1 canisters arranged in the configuration sketched in figure 6. The source characteristics used in the model were those as reported

in EOSAEL 80 Technical Documentation;²³ and the mass extinction coefficient, single scattering albedo, and phase function were those of Shirkey, Clayton, and Quintis²⁸ for HC smoke. For modeling purposes, the munitions were separated into four groups as indicated by the sketched outlines in figure 6 with each group treated as single-point detonation of appropriate total mass. For buoyant smokes this latter procedure may cause some concern; however, for HC munitions which are only slightly buoyant this procedure causes only insignificant errors.

Meteorological conditions during the test were typical of fair weather with 30 percent cloud cover and 11.3 km visibility. Model inputs either taken from the original test report or derived (estimated) from data therein are listed in table 2. Table 3 lists the ambient sky radiation measurements made during these tests.

The sky radiance map derived from the data of table 3 for the model sector midpoints is shown in figure 7.

Figure 8 shows the modeled and measured results for both path integrated concentration (figure 8a) and path luminance (figure 8b). The results for path integrated concentration, although overall high, are typical of those reported in other validation studies.²⁹ The path luminance results are most interesting in that the brightening effect at the cloud edges is quite noticeable. This effect is often observed in natural clouds and is referred to as a "silver lining." The occurrence and magnitude of the bright edges depend strongly upon the angular distribution of ambient radiation. The overall agreement between model data and data of figure 8b is encouraging.

Figure 9 is a more detailed examination of the cloud at time $t = 100$ s. Here both the direct and diffuse components of radiation are plotted as a function of depth of penetration. This procedure may be viewed as moving the target into the cloud along the LOS away from the observer. Until a significant portion of the cloud is penetrated, the diffuse component is near zero and the

²³R. A. Sutherland, 1981, "Smoke Obscuration Model," chapter 3, EOSAEL 80, Volume 1, Technical Documentation, editor L. D. Duncan, ASL-TR-0072, US Army Atmospheric Sciences Laboratory, White Sands Missile Range, NM (AD B055130L)

²⁸R. C. Shirkey, D. Clayton, and D. M. Quintis, 1981, "Aerosol Phase Function Data File PFNDAT," chapter 16, EOSAEL 80, Volume II, Users Manual, editors R. C. Shirkey and S. G. O'Brien, ASL-TR-0073, US Army Atmospheric Sciences Laboratory, White Sands Missile Range, NM (AD B056119)

²⁹D. W. Hoock, R. A. Sutherland, and D. Clayton, 1981, Comparisons Between the EOSAEL 80 Model SMOKE and the Inventory Munition Test Phase IIa, Technical Report, US Army Atmospheric Sciences Laboratory, White Sands Missile Range, NM (in process)

direct component is at a maximum. As the target moves into the cloud, the diffuse component increases while the direct component decreases. The net effect is a reduction in both the direct signal and the contrast.

A discussion of how these (and other) outputs of the model can be used in other smoke screening and perception models can be found elsewhere.³⁰

³⁰D. W. Hoock and R. A. Sutherland, 1981, "Path to Background Luminance Ratios for the EOSAEL 80 Munitions Expenditure Model SCREEN," Proceedings of Smoke Symposium V, Harry Diamond Laboratories, Adelphi, MD

TABLE 1. DIFFUSION PARAMETERS USED IN THE TRANSPORT AND DIFFUSION ROUTINE FOR VARIOUS VALUES OF ROUGHNESS PARAMETER (Z_0) AND STABILITY CATEGORY.*

		STABILITY CATEGORY					
		A	B	C	D	E	F
Default	A_x	7.57	7.57	7.57	7.57	7.57	7.57
	B_x	0.93	0.93	0.93	0.93	0.93	0.93
	A_y	44.1	44.1	44.1	24.8	15.6	15.6
	B_y	1.50	1.50	1.50	0.88	0.66	0.66
	A_z	16.4	16.4	16.4	14.2	12.7	12.7
	B_z	1.50	1.50	1.50	0.88	0.66	0.66
	$0 \leq Z_0 < 10$	A_x	2.77	3.55	5.38	8.68	12.6
B_x		0.90	0.90	0.90	0.90	0.90	0.90
A_y		2.77	3.55	5.38	8.68	12.6	17.5
B_y		0.90	0.90	0.90	0.90	0.90	0.90
A_z		7.32	9.65	12.0	15.6	26.3	47.6
B_z		0.94	0.89	0.85	0.81	0.78	0.72
$10 \leq Z_0 < 100$		A_x	2.77	3.55	5.38	8.68	12.6
	B_x	0.90	0.90	0.90	0.90	0.90	0.90
	A_y	2.77	3.55	5.38	8.68	12.6	17.5
	B_y	0.90	0.90	0.90	0.90	0.90	0.90
	A_z	4.13	5.78	6.75	8.59	14.9	24.6
	B_z	0.90	0.85	0.80	0.76	0.73	0.67
	$Z_0 > 100$	A_x	2.77	3.55	5.38	8.68	12.6
B_x		0.90	0.90	0.90	0.90	0.90	0.90
A_y		2.77	3.55	5.38	8.68	12.6	17.5
B_y		0.90	0.90	0.90	0.90	0.90	0.90
A_z		1.80	2.23	2.40	3.17	5.07	7.57
B_z		0.83	0.77	0.72	0.68	0.65	0.58

* Z_0 in centimeters, x, y, and z in meters.

TABLE 2. AMBIENT RADIATION MEASUREMENTS (VISIBLE) FROM SMOKE WEEK II, TRIAL 1
FIELD TEST.*

$\phi \rightarrow$ $\theta \downarrow$	Sky Radiance $W\ sr^{-1}\ m^{-2}$			
	<u>3.7°</u>	<u>70.7°</u>	<u>160.7°</u>	<u>250.7°</u>
0°	6.2	6.2	6.2	6.2
10°	9.8	12.1	15.8	13.1
20°	7.5	13.1	20.7	13.1
30°	6.6	5.1	33.8	13.1
40°	7.5	17.4	54.5	12.1
50°	8.5	19.7	133.6	13.1
60°	10.8	21.3	124.7	13.1
70°	13.1	21.3	124.7	17.4
80°	17.4	10.8	103.4	17.4
90°	18.4	8.9	68.6	18.1

Solar:

Zenith	Azimuth	Beam flux (W/m^2)
51.5	151.9	208.7

Surface Irradiance (W/m^2): 571.5

*Note that reported sky radiance data must be divided by $(\pi/180)^2$ to convert unit solid angle to 1 sr. Also a factor 10^{-2} converts $\mu W/cm^2$ to W/m^2

TABLE 3. METEOROLOGICAL INPUTS TO THE MODEL FOR
SMOKE WEEK II, TRIAL 1 FIELD TEST

Windspeed (8 m)	4.1 m/s
Wind direction (8 m)	116.3 deg
Wind power law exponent	0.11
Ambient air temperature (1.0 m)	23.6°C
Temperature gradient	-0.36°C/m
Mixing height	400 m (derived in model)
Mixing height temperature	18.3°C (derived in model)
Stability category (Pasquill)	C
Relative humidity	52%
Dew-point temperature	not needed
Surface irradiance (short wave)	0.82 Langley/min
Surface temperature	24.0°C (derived in model)
Surface reflectivity	0.25 (estimated from data)
Surface roughness	0.0 (default)
Surface particle reflectance	1.0 (default)

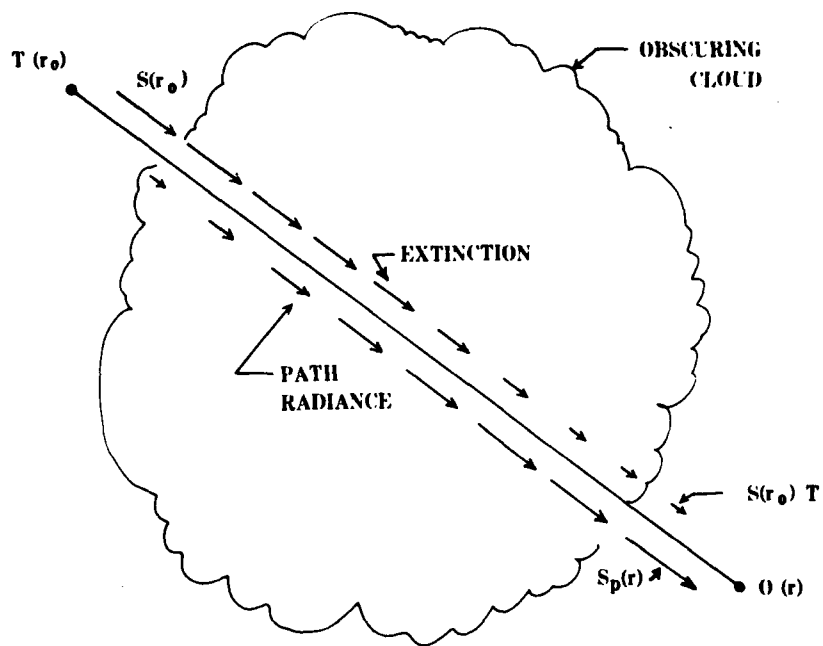


Figure 1. Sketch demonstrating the effects of extinction and path radiance on radiant energy received by an observer.

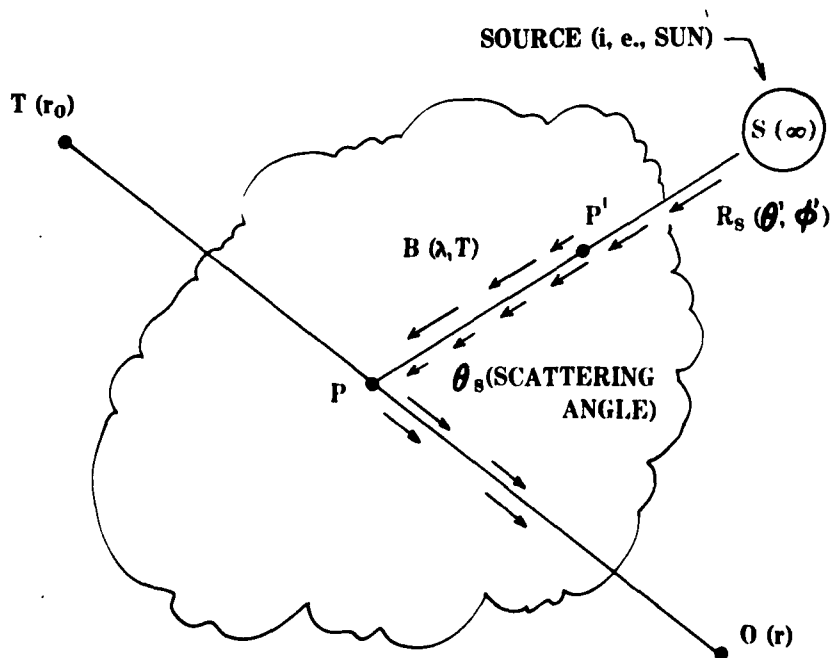


Figure 2. Sketch demonstrating the scattering of ambient radiation into the LOS.

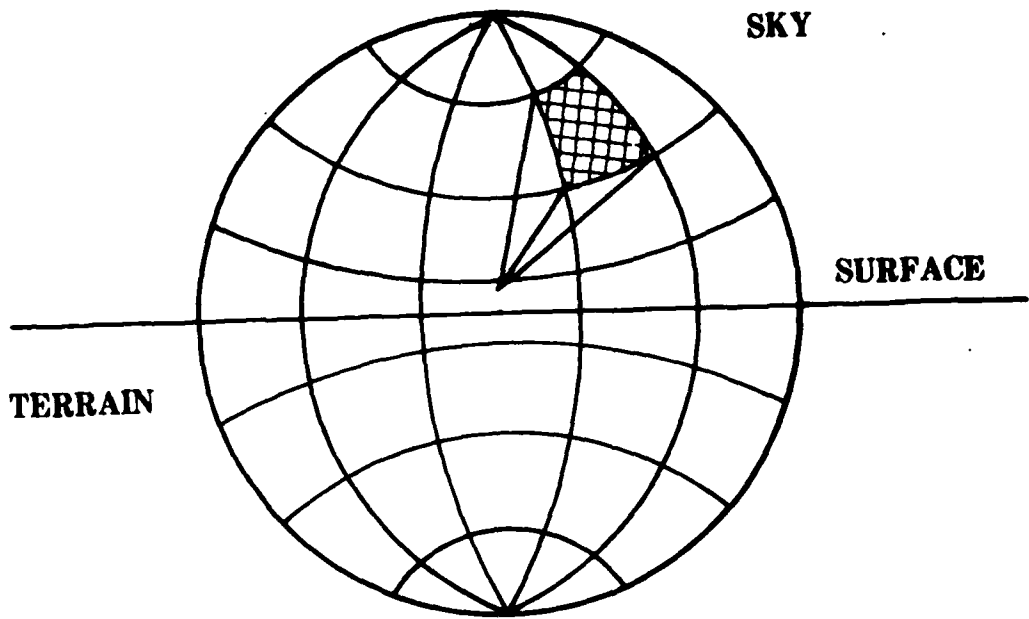


Figure 3. Sketch demonstrating the sky/terrain sectoring scheme used in the model.

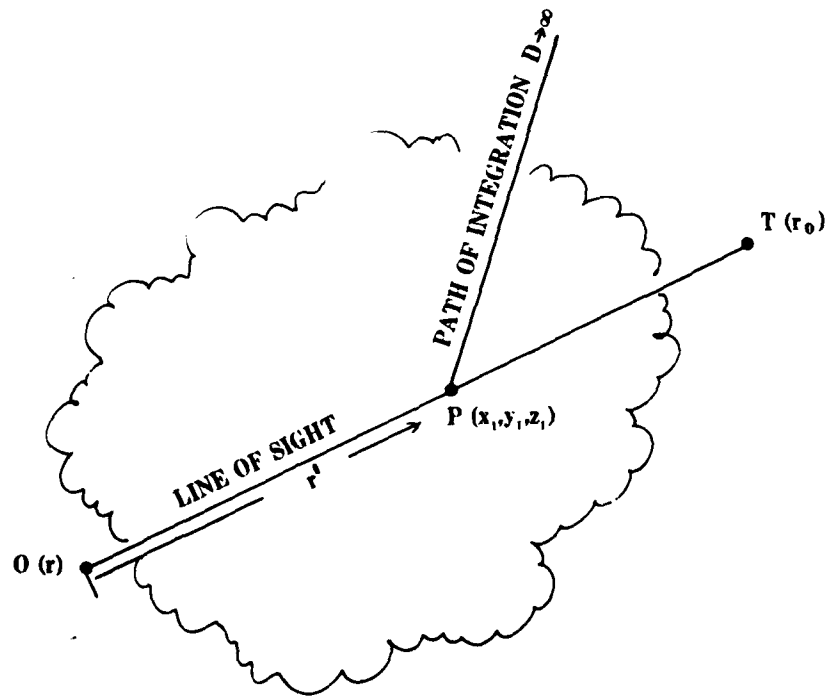


Figure 4. Sketch demonstrating the geometry for computing optical thickness.

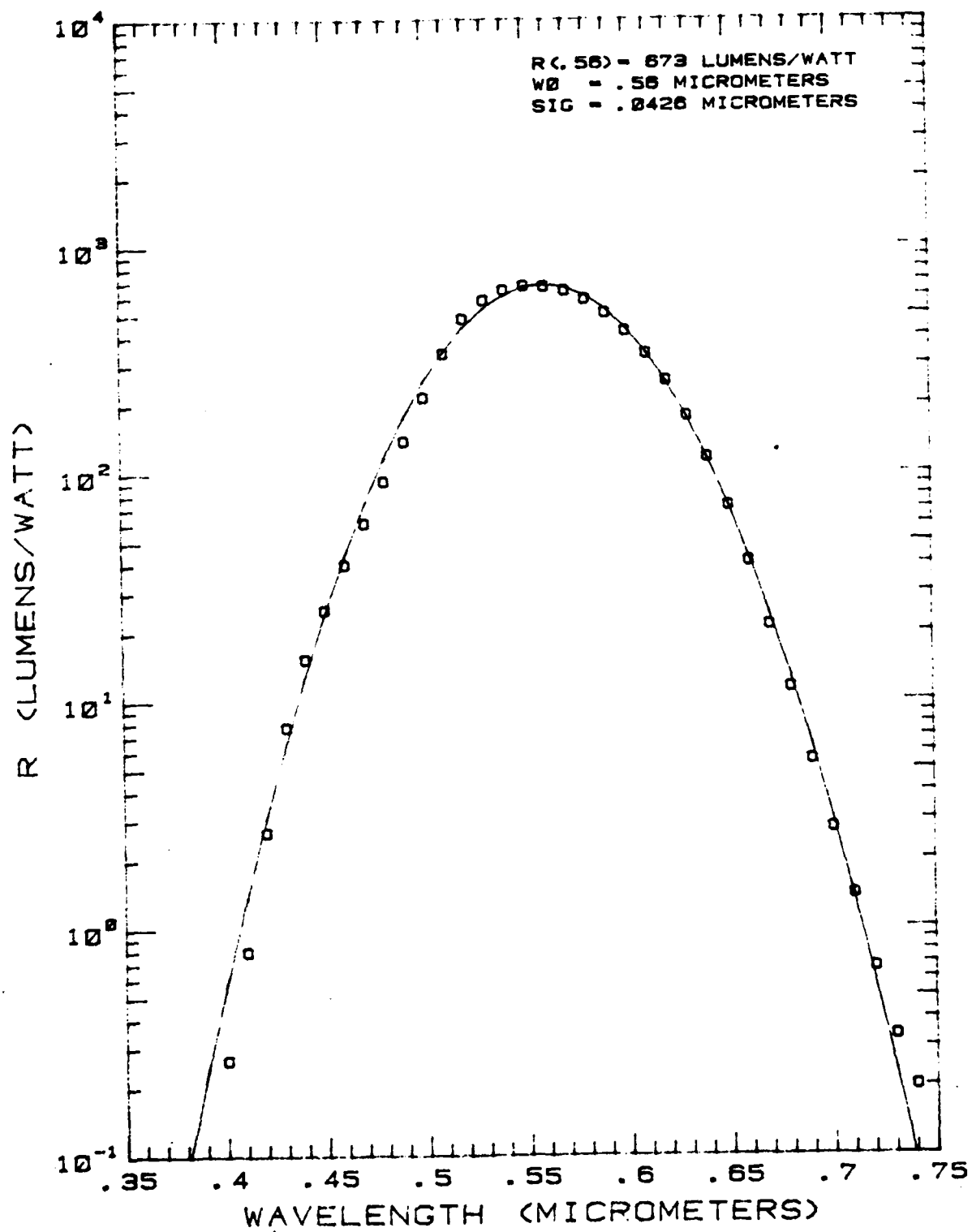


Figure 5. Photopic response curve and Gaussian functional fit for converting radiance (W/m^2) to luminance (candies/m^2).

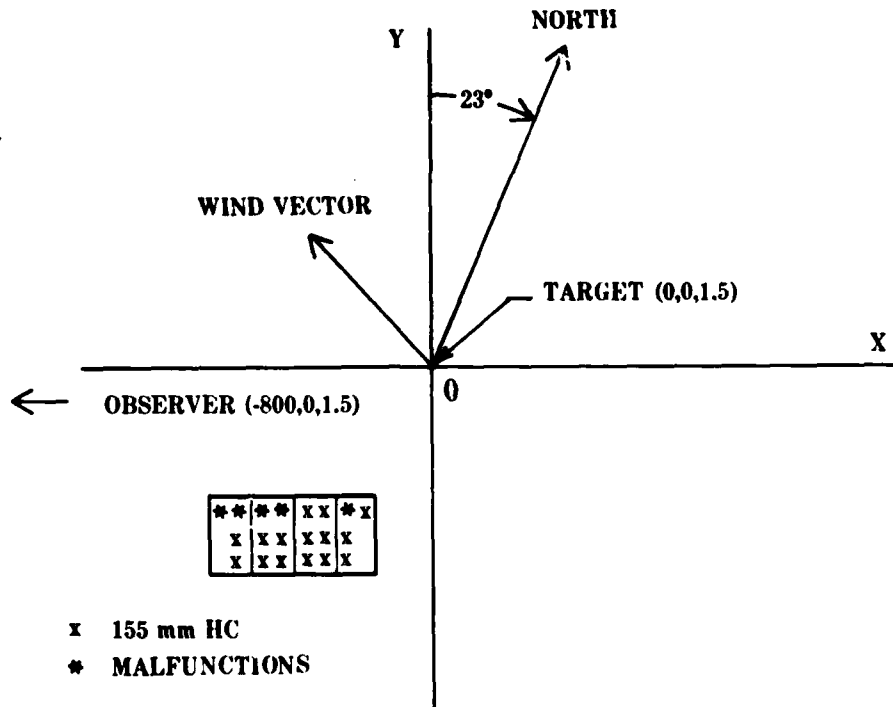


Figure 6. Test configuration for Smoke Week II, Trial 1 Field Test.

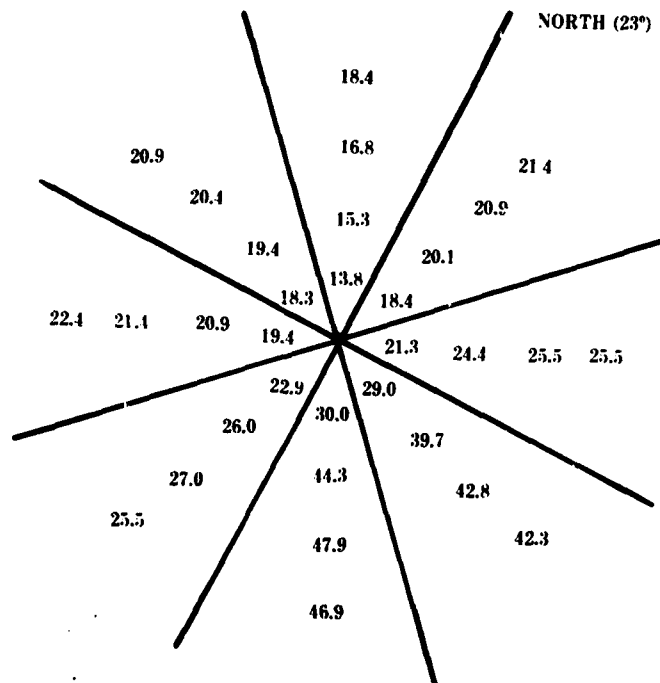


Figure 7. Sky radfance map $W/(sr \cdot m^2)$ as derived from Smoke Week II, Trial 1 Field Test.

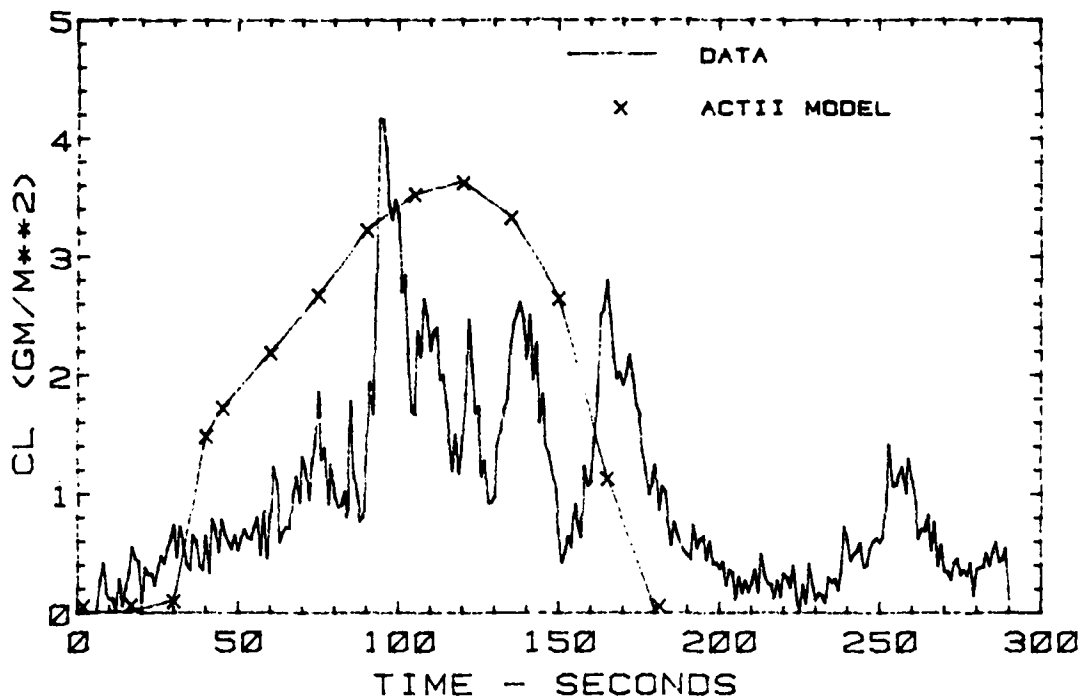


FIGURE 8a. TRIAL 01 SMOKE WEEK II
 Results of comparisons of path integrated concentration

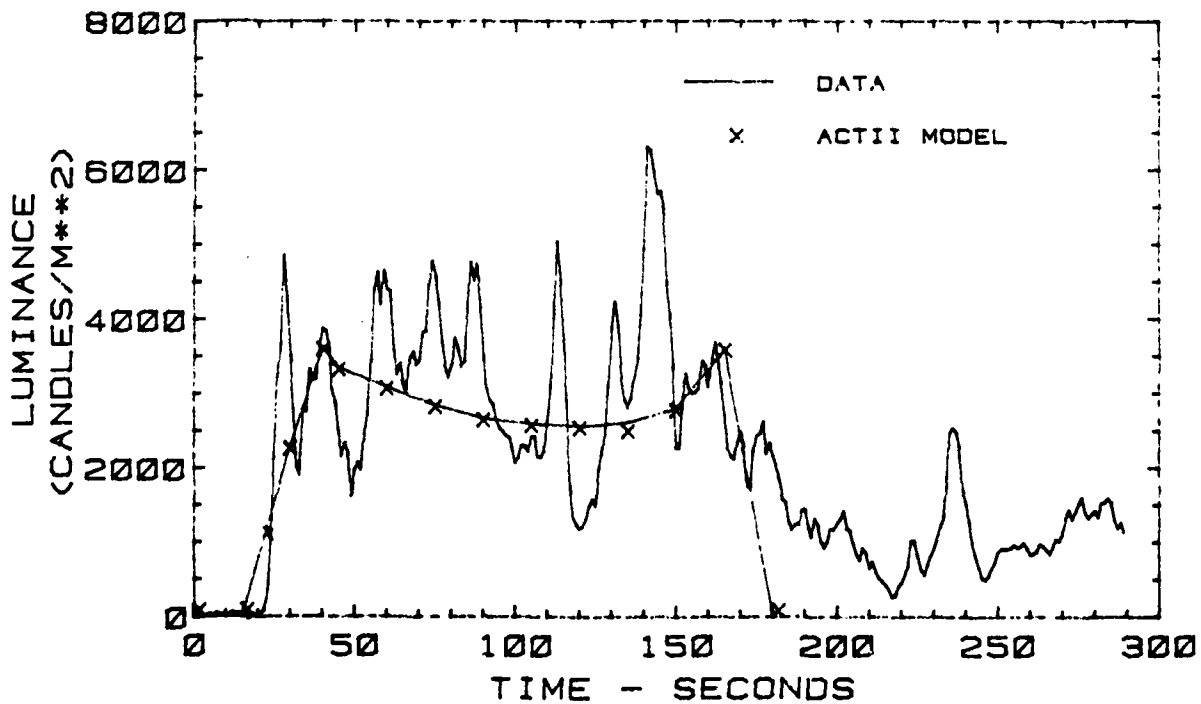


FIGURE 8b. TRIAL 01 SMOKE WEEK II
 Results of comparisons for path brightness

Figure 8. Model comparisons of path integrated concentration (CL) and path luminance with data from Smoke Week II, Trial 1 Field Test.

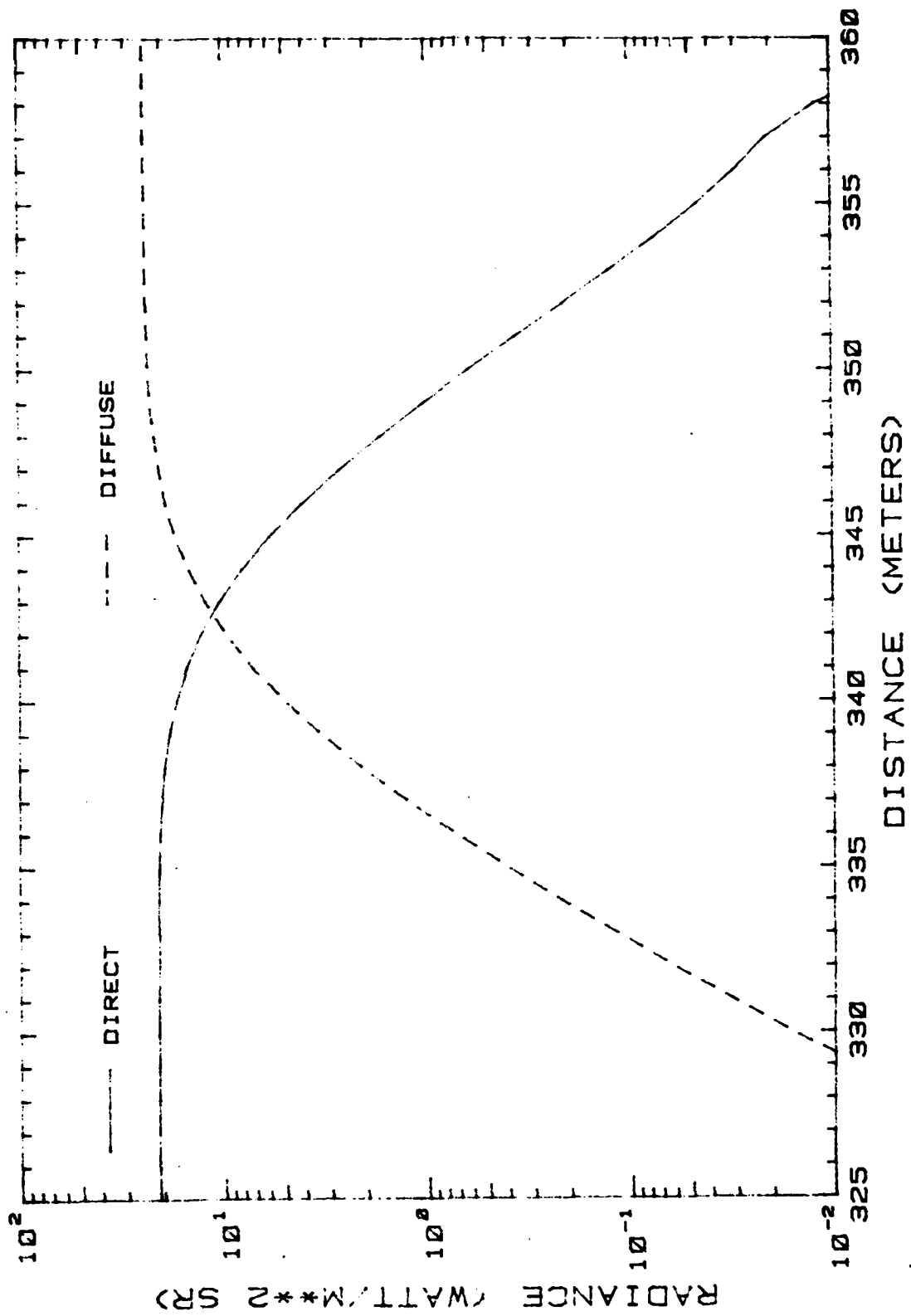


Figure 9. Modeled diffuse and direct radiation as a function of target position along the LOS.

REFERENCES

1. Sutherland, R. A., D. W. Hoock, and R. B. Gomez, 1981, An Objective Summary of US Army Electro-Optical Modeling and Field Testing in an Obscurant Environment, ASL-TR-0096, US Army Atmospheric Sciences Laboratory White Sands Missile Range, NM.
2. Sutherland, R. A., et al: 1979, "A Real Time Satellite Data Acquisition, Analysis and Display System-A Practical Application of the GOES Network," J Appl Meteorol, 3:355-360.
3. Chen, E., et al, 1979, "Satellite-Sensed Winter Nocturnal Temperature Patterns of the Everglades Agricultural Area," J Appl Meteorol, 8:992-1002.
4. Kern, C. D., 1965, "Evaluation of Infrared Emission of Clouds and Ground as Measured by Weather Satellites," Environmental Research Papers, No. 155, AFCRL-65-840, Air Force Cambridge Research Laboratories, Hanscom Air Force Base, MA.
5. Greenfield, S. M., and W. W. Kellogg, 1960, "Calculations of Atmospheric Infrared Radiation as seen from a Meteorological Satellite," J Meteorol, 6:283-290.
6. Shirkey, R. C., and R. A. Sutherland, 1981, "Aerosol Phase Function Data Base," chapter 16, EOSAEL 80, Volume I, Technical Documentation, editor L. D. Duncan, ASL-TR-0072, US Army Atmospheric Sciences Laboratory, White Sands Missile Range, NM. (AD B055130L)
7. Smoke Obscuration Model II (SOM II) Computer Code Volume II - Analyst Manual, 1979, JTCG/ME Smoke and Aerosol Working Group Document 61, JTCG/ME-78-9-2.
8. Dumbauld, R. K., and H. Bjorklund, 1977, Mixing Layer Analysis Routine and Transport/Diffusion Application Routine for EPAMS, ECOM-77-2, Atmospheric Sciences Laboratory, US Army Electronics Command, White Sands Missile Range, NM.
9. Gomez, R. B., R. Pennsyle, and D. Stadlander, 1979, "Battlefield Obscuration Model, ACT I," Proceedings of Smoke Symposium III, Harry Diamond Laboratories, Adelphi, MD.
10. "Combat Simulation Target Acquisition Model and Data Input" (U), CONFIDENTIAL, 1980, Draft Technical Report, US Army Night Vision and Electro-Optics Laboratory, Fort Belvoir, VA. (in process)
11. Pennsyle, R. O., 1979, Methodology for Estimating Smoke/Obscurant Munition Expenditure Requirements, ARCSL-TR-79022, Chemical Systems Laboratory, Aberdeen Proving Ground, MD.

12. Hoock, D. W., 1981, "SCREEN," chapter 5, EOSAEL 80, Volume 1, Technical Documentation, editor L. D. Duncan, ASL-TR-0072, US Army Atmospheric Sciences Laboratory, White Sands Missile Range, NM. (AD B055130L)
13. Selby, J. E., et al, 1978, "Atmospheric Transmittance/Radiance: Computer Code LOWTRAN 4," Environmental Research Papers, No. 626, AFGL-TR-78-0053, Air Force Geophysics Laboratory, Hanscom Air Force Base, MA.
14. Shirkey, R. C., et al, 1980, Single Scattering Code AGAUSX: Theory, Applications, Comparisons, and Listing, ASL-TR-0062, US Army Atmospheric Sciences Laboratory, White Sands Missile Range, NM.
15. DPG Final Test Report on Smoke Week II at Eglin AFB, FL (U), CONFIDENTIAL, 1978, Volumes I and II, DPG-FR-78-317, Dugway Proving Ground, UT.
16. Smoke Effectiveness Manual, 1979, JTCG/ME Smoke and Aerosol Working Group Document Number FM 101-61-8.
17. Hansen, F. V., 1979, Engineering Estimates for the Calculation of Atmospheric Dispersion Coefficients, ASL Internal Report, US Army Atmospheric Sciences Laboratory, White Sands Missile Range, NM.
18. Pasquill, F., 1974, Atmospheric Diffusion, second edition, Halsted Press Div., John Wiley and Sons, Inc., New York.
19. Priestley, C. H. B., 1956, "A Working Theory of the Bent-Over Plume of Hot Gas," Quart J Roy Meteorol Soc, 82:165-176.
20. Sutherland, R. A., and D. Clayton, 1981, An Improved Smoke Obscuration Model Act II: Part 2 Documentation and User Guide, Technical Report, US Army Atmospheric Sciences Laboratory, White Sands Missile Range, NM. (in process)
21. Sutherland, R. A., 1981, "Comparisons Between the Improved Smoke Obscuration Model ACT II and Recent Smoke Week Data," Proceedings of Smoke Symposium V, Harry Diamond Laboratories, Adelphi, MD.
22. Chandrasekhar, S., 1960, Radiative Transfer, second edition, Dover Press Publications, Inc., New York.
23. Sutherland, R. A., 1981, "Smoke Obscuration Model," chapter 3, EOSAEL 80, Volume 1, Technical Documentation, editor L. D. Duncan, ASL-TR-0072, US Army Atmospheric Sciences Laboratory, White Sands Missile Range, NM. (AD B055130L)
24. Abramowitz, M., and I. Stegun, 1970, Handbook of Mathematical Functions, Dover Press Publications, Inc., New York.

25. Analysis of the Smoke Cloud Data from the August 1975 Jefferson Proving Ground Smoke Test, 1977, AMSAA Technical Report TR-201, Aberdeen Proving Ground, MD. (AD A045874)
26. Briggs, G. A., 1965, "A Plume Rise Model Compared with Observations," J Air Poll Control Assoc, 15:433.
27. Stimson, A., 1974, Photometry and Radiometry for Engineers, John Wiley and Sons, Inc., New York.
28. Shirkey, R. C., D. Clayton, and D. M. Quintis, 1981, "Aerosol Phase Function Data File PFNDAT," chapter 16, EOSAEL 80, Volume II, Users Manual, editors R. C. Shirkey and S. G. O'Brien, ASL-TR-0073, US Army Atmospheric Sciences Laboratory, White Sands Missile Range, NM. (AD B056119)
29. Hoock, D. W., R. A. Sutherland, and D. Clayton, 1981, Comparisons Between the EOSAEL 80 Model SMOKE and the Inventory Munition Test Phase IIa, Technical Report, US Army Atmospheric Sciences Laboratory, White Sands Missile Range, NM. (in process)
30. Hoock, D. W., and R. A. Sutherland, 1981, "Path to Background Luminance Ratios for the EOSAEL 80 Munitions Expenditure Model SCREEN," Proceedings of Smoke Symposium V, Harry Diamond Laboratories, Adelphi, MD.

ELECTRO-OPTICS DISTRIBUTION LIST

Commander
US Army Aviation School
Fort Rucker, AL 36362

Commander
US Army Aviation Center
ATTN: ATZQ-D-MA (Mr. Oliver N. Heath)
Fort Rucker, AL 36362

Commander
US Army Aviation Center
ATTN: ATZQ-D-MS (Mr. Donald Wagner)
Fort Rucker, AL 36362

NASA/Marshall Space Flight Center
ATTN: ES-83 (Otha H. Vaughan, Jr.)
Huntsville, AL 35812

NASA/Marshall Space Flight Center
Atmospheric Sciences Division
ATTN: Code ES-81 (Dr. William W. Vaughan)
Huntsville, AL 35812

Nichols Research Corporation
ATTN: Dr. Lary W. Pinkley
4040 South Memorial Parkway
Huntsville, AL 35802

John M. Hobbie
c/o Kentron International
2003 Byrd Spring Road
Huntsville, AL 35802

Mr. Ray Baker
Lockheed-Missile & Space Company
4800 Bradford Blvd
Huntsville, AL 35807

Commander
US Army Missile Command
ATTN: DRSMI-OG (Mr. Donald R. Peterson)
Redstone Arsenal, AL 35809

Commander
US Army Missile Command
ATTN: DRSMI-OGA (Dr. Bruce W. Fowler)
Redstone Arsenal, AL 35809

Commander
US Army Missile Command
ATTN: DRSMI-REL (Dr. George Emmons)
Redstone Arsenal, AL 35809

Commander
US Army Missile Command
ATTN: DRSMI-REO (Huey F. Anderson)
Redstone Arsenal, AL 35809

Commander
US Army Missile Command
ATTN: DRSMI-REO (Mr. Maxwell W. Harper)
Redstone Arsenal, AL 35809

Commander
US Army Missile Command
ATTN: DRSMI-REO (Mr. Gene Widenhofer)
Redstone Arsenal, AL 35809

Commander
US Army Missile Command
ATTN: DRSMI-RHC (Dr. Julius Q. Lilly)
Redstone Arsenal, AL 35809

Commander
US Army Missile Command
Redstone Scientific Information Center
ATTN: DRSMI-RPRD (Documents Section)
Redstone Arsenal, AL 35809

Commander
US Army Missile Command
ATTN: DRSMI-RRR (Dr. Oskar Essenwanger)
Redstone Arsenal, AL 35809

Commander
US Army Missile Command
ATTN: DRSMI-RRR (Mr. Charles Christensen)
Redstone Arsenal, AL 35809

Commander
US Army Missile Command
ATTN: DRSMI-RRR (Dr. George A. Tanton)
Redstone Arsenal, AL 35809

Commander
US Army Communications Command
ATTN: CC-OPS-PP
Fort Huachuca, AZ 85613

Commander
US Army Intelligence Center & School
ATTN: ATSI-CD-CS (Mr. Richard G. Cundy)
Fort Huachuca, AZ 85613

Commander
US Army Intelligence Center & School
ATTN: ATSI-CD-MD (Mr. Harry Wilder)
Fort Huachuca, AZ 85613

Commander
US Army Intelligence Center & School
ATTN: ATSI-CS-C (2LT Coffman)
Fort Huachuca, AZ 85613

Commander
US Army Yuma Proving Ground
ATTN: STEYP-MSA-TL
Bldg 2105
Yuma, AZ 85364

Northrop Corporation
Electro-Mechanical Division
ATTN: Dr. Richard D. Tooley
500 East Orangethorpe Avenue
Anaheim, CA 92801

Commander
Naval Weapons Center
ATTN: Code 3918 (Dr. Alexis Shlanta)
China Lake, CA 93555

Hughes Helicopters
Army Advanced Attack Helicopter Weapons
ATTN: Mr. Charles R. Hill
Centinela and Teale Streets
Bldg 305, MS T-73A
Culter City, CA 90230

Commander
US Army Combat Developments
Experimentation Command
ATTN: ATEC-PL-M (Mr. Gary G. Love)
Fort Ord, CA 93941

SRI International
ATTN: K2060/Dr. Edward E. Uthe
333 Ravenswood Avenue
Menlo Park, CA 94025

SRI International
ATTN: Mr. J. E. Van der Laan
333 Ravenswood Avenue
Menlo Park, CA 94025

Joane May
Naval Environmental Prediction
Research Facility (NEPRF)
ATTN: Library
Monterey, CA 93940

Sylvania Systems Group,
Western Division
GTE Products Corporation
ATTN: Technical Reports Library
P.O. Box 205
Mountain View, CA 94042

Sylvania Systems Group
Western Division
GTE Products Corporation
ATTN: Mr. Lee W. Carrier
P.O. Box 188
Mountain View, CA 94042

Pacific Missile Test Center
Geophysics Division
ATTN: Code 3250-3 (R. de Violini)
Point Mugu, CA 93042

Pacific Missile Test Center
Geophysics Division
ATTN: Code 3253 (Terry E. Battalino)
Point Mugu, CA 93042

Effects Technology Inc.
ATTN: Mr. John D. Carlyle
5383 Hollister Avenue
Santa Barbara, CA 93111

Commander
Naval Ocean Systems Center
ATTN: Code 532 (Dr. Juergen Richter)
San Diego, CA 92152

Commander
Naval Ocean Systems Center
ATTN: Code 5322 (Mr. Herbert G. Hughes)
San Diego, CA 92152

Commander
Naval Ocean Systems Center
ATTN: Code 4473 (Tech Library)
San Diego, CA 92152

The RAND Corporation
ATTN: Ralph Huschke
1700 Main Street
Santa Monica, CA 90406

Particle Measuring Systems, Inc.
ATTN: Dr. Robert G. Knollenberg
1855 South 57th Court
Boulder, CO 80301

US Department of Commerce
National Oceanic and Atmospheric Admin
Environmental Research Laboratories
ATTN: Library, R-51, Technical Reports
325 Broadway
Boulder, CO 80303

US Department of Commerce
National Oceanic and Atmospheric Admin
Environmental Research Laboratories
ATTN: R45X3 (Dr. Vernon E. Derr)
Boulder, CO 80303

US Department of Commerce
National Telecommunications and
Information Administration
Institute for Telecommunication Sciences
ATTN: Code 1-3426 (Dr. Hans J. Liebe)
Boulder, CO 80303

AFATL/DLODL
Technical Library
Eglin AFB, FL 32542

Commanding Officer
Naval Training Equipment Center
ATTN: Technical Information Center
Orlando, FL 32813

Georgia Institute of Technology
Engineering Experiment Station
ATTN: Dr. Robert W. McMillan
Atlanta, GA 30332

Georgia Institute of Technology
Engineering Experiment Station
ATTN: Dr. James C. Wiltse
Atlanta, GA 30332

Commandant
US Army Infantry Center
ATTN: ATSH-CD-MS-E (Mr. Robert McKenna)
Fort Benning, GA 31805

Commander
US Army Signal Center & Fort Gordon
ATTN: ATZHCD-CS
Fort Gordon, GA 30905

Commander
US Army Signal Center & Fort Gordon
ATTN: ATZHCD-O
Fort Gordon, GA 30905

USAFETAC/DNE
ATTN: Mr. Charles Glauber
Scott AFB, IL 62225

Commander
Air Weather Service
ATTN: AWS/DNDP (LTC Kit G. Cottrell)
Scott AFB, IL 62225

Commander
Air Weather Service
ATTN: AWS/DOOF (MAJ Robert Wright)
Scott AFB, IL 62225

Commander
US Army Combined Arms Center
& Ft. Leavenworth
ATTN: ATZLCA-CAA-Q (Mr. H. Kent Pickett)
Fort Leavenworth, KS 66027

Commander
US Army Combined Arms Center
& Ft. Leavenworth
ATTN: ATZLCA-SAN (Robert DeKinder, Jr.)
Fort Leavenworth, KS 66027

Commander
US Army Combined Arms Center
& Ft. Leavenworth
ATTN: ATZLCA-SAN (Mr. Kent I. Johnson)
Fort Leavenworth, KS 66027

Commander
US Army Combined Arms Center
& Ft. Leavenworth
ATTN: ATZLCA-WE (LTC Darrell Holland)
Fort Leavenworth, KS 66027

President
USAARENBD
ATTN: ATZK-AE-TA (Dr. Charles R. Leake)
Fort Knox, KY 40121

Commander
US Army Armor Center and Fort Knox
ATTN: ATZK-CD-MS
Fort Knox, KY 40121

Commander
US Army Armor Center and Fort Knox
ATTN: ATZK-CD-SD
Fort Knox, KY 40121

Aerodyne Research Inc.
ATTN: Dr. John F. Ebersole
Crosby Drive
Bedford, MA 01730

Commander
Air Force Geophysics Laboratory
ATTN: OPA (Dr. Robert W. Fenn)
Hanscom AFB, MA 01731

Commander
Air Force Geophysics Laboratory
ATTN: OPI (Dr. Robert A. McClatchey)
Hanscom AFB, MA 01731

Massachusetts Institute of Technology
Lincoln Laboratory
ATTN: Dr. T. J. Goblick, B-370
P.O. Box 73
Lexington, MA 02173

Massachusetts Institute of Technology
Lincoln Laboratory
ATTN: Dr. Michael Gruber
P.O. Box 73
Lexington, MA 02173

Raytheon Company
Equipment Division
ATTN: Dr. Charles M. Sonnenschein
430 Boston Post Road
Wayland, MA 01778

Commander
US Army Ballistic Research Laboratory/
ARRADCOM
ATTN: DRDAR-BLB (Mr. Richard McGee)
Aberdeen Proving Ground, MD 21005

Commander/Director
Chemical Systems Laboratory
US Army Armament Research
& Development Command
ATTN: DRDAR-CLB-PS (Dr. Edward Stuebing)
Aberdeen Proving Ground, MD 21010

Commander/Director
Chemical Systems Laboratory
US Army Armament Research
& Development Command
ATTN: DRDAR-CLB-PS (Mr. Joseph Vervier)
Aberdeen Proving Ground, MD 21010

Commander/Director
Chemical Systems Laboratory
US Army Armament Research
& Development Command
ATTN: DRDAR-CLY-A (Mr. Ronald Pennsyle)
Aberdeen Proving Ground, MD 21010

Commander
US Army Ballistic Research Laboratory/
ARRADCOM
ATTN: DRDAR-TSB-S (STINFO)
Aberdeen Proving Ground, MD 21005

Commander
US Army Electronics Research
& Development Command
ATTN: DRDEL-CCM (W. H. Pepper)
Adelphi, MD 20783

Commander
US Army Electronics Research
& Development Command
ATTN: DRDEL-CG/DRDEL-DC/DRDEL-CS
2800 Powder Mill Road
Adelphi, MD 20783

Commander
US Army Electronics Research
& Development Command
ATTN: DRDEL-CT
2800 Powder Mill Road
Adelphi, MD 20783

Commander
US Army Electronics Research
& Development Command
ATTN: DRDEL-PAO (M. Singleton)
2800 Powder Mill Road
Adelphi, MD 20783

Project Manager
Smoke/Obscurants
ATTN: DRDPM-SMK
(Dr. Anthony Van de Wal, Jr.)
Aberdeen Proving Ground, MD 21005

Project Manager
Smoke/Obscurants
ATTN: DRDPM-SMK-T (Mr. Sidney Gerard)
Aberdeen Proving Ground, MD 21005

Commander
US Army Test & Evaluation Command
ATTN: DRSTE-AD-M (Mr. Warren M. Baity)
Aberdeen Proving Ground, MD 21005

Commander
US Army Test & Evaluation Command
ATTN: DRSTE-AD-M (Dr. Norman E. Pentz)
Aberdeen Proving Ground, MD 21005

Director
US Army Materiel Systems Analysis Activity
ATTN: DRXSY-AAM (Mr. William Smith)
Aberdeen Proving Ground, MD 21005

Director
US Army Materiel Systems Analysis Activity
ATTN: DRXSY-CS (Mr. Philip H. Beavers)
Aberdeen Proving Ground, MD 21005

Director
US Army Materiel Systems Analysis Activity
ATTN: DRXSY-GB (Wilbur L. Warfield)
Aberdeen Proving Ground, MD 21005

Director
US Army Materiel Systems Analysis Activity
ATTN: DRXSY-GP (Mr. Fred Campbell)
Aberdeen Proving Ground, MD 21005

Director
US Army Materiel Systems Analysis Activity
ATTN: DRXSY-GP (H. Stamper)
Aberdeen Proving Grounds, MD 21005

Director
US Army Materiel Systems Analysis Activity
ATTN: DRXSY-GS
(Mr. Michael Starks/Mr. Julian Chernick)
Aberdeen Proving Ground, MD 21005

Director
US Army Materiel Systems Analysis Activity
ATTN: DRXSY-J (Mr James F. O'Bryon)
Aberdeen Proving Ground, MD 21005

Director
US Army Materiel Systems Analysis Activity
ATTN: DRXSY-LM (Mr. Robert M. Marchetti)
Aberdeen Proving Ground, MD 21005

Commander
Harry Diamond Laboratories
ATTN: Dr. William W. Carter
2800 Powder Mill Road
Adelphi, MD 20783

Commander
Harry Diamond Laboratories
ATTN: DELHD-R-CM (Mr. Robert McCoskey)
2800 Powder Mill Road
Adelphi, MD 20783

Commander
Harry Diamond Laboratories
ATTN: DELHD-R-CM-NM (Dr. Robert Humphrey)
2800 Powder Mill Road
Adelphi, MD 20783

Commander
Harry Diamond Laboratories
ATTN: DELHD-R-CM-NM (Dr. Z. G. Sztankay)
2800 Powder Mill Road
Adelphi, MD 20783

Commander
Harry Diamond Laboratories
ATTN: DELHD-R-CM-NM (Dr. Joseph Nemarich)
2800 Powder Mill Road
Adelphi, MD 20783

Commander
Air Force Systems Command
ATTN: WER (Mr. Richard F. Picanso)
Andrews AFB, MD 20334

Martin Marietta Laboratories
ATTN: Jar Mo Chen
1450 South Rolling Road
Baltimore, MD 21227

Commander
US Army Concepts Analysis Agency
ATTN: CSCA-SMC (Mr. Hal E. Hock)
8120 Woodmont Avenue
Bethesda, MD 20014

Director
National Security Agency
ATTN: R52/Dr. Douglas Woods
Fort George G. Meade, MD 20755

Chief
Intelligence Materiel Development
& Support Office
US Army Electronic Warfare Laboratory
ATTN: DELEW-I (LTC Kenneth E. Thomas)
Fort George G. Meade, MD 20755

The Johns Hopkins University
Applied Physics Laboratory
ATTN: Dr. Michael J. Lun
John Hopkins Road
Laurell, MD 20810

Dr. Stephen T. Hanley
1720 Rhodesia Avenue
Oxon Hill, MD 20022

Science Applications Inc.
ATTN: Mr. G. D. Currie
15 Research Drive
Ann Arbor, MI 48103

Science Applications Inc.
ATTN: Dr. Robert E. Turner
15 Research Drive
Ann Arbor, MI 48103

Commander
US Army Tank-Automotive Research
& Development Command
ATTN: DRDTA-ZSC (Mr. Harry Young)
Warren, MI 48090

Commander
US Army Tank Automotive Research
& Development Command
ATTN: DRDTA-ZSC (Mr. Wallace Mick, Jr.)
Warren, MI 48090

Dr. A. D. Belmont
Research Division
Control Data Corporation
P.O. Box 1249
Minneapolis, MN 55440

Director
US Army Engr Waterways Experiment Station
ATTN: WESEN (Mr. James Mason)
P.O. Box 631
Vicksburg, MS 39180

Dr. Jerry Davis
Department of Marine, Earth
and Atmospheric Sciences
North Carolina State University
Raleigh, NC 27650

Commander
US Army Research Office
ATTN: DRXRO-GS (Dr. Leo Alpert)
P.O. Box 12211
Research Triangle Park, NC 27709

Commander
US Army Research Office
ATTN: DRXRO-PP (Brenda Mann)
P.O. Box 12211
Research Triangle Park, NC 27709

Commander
US Army Cold Regions Research
& Engineering Laboratory
ATTN: CRREL-RD (Dr. K. F. Sterrett)
Hanover, NH 03755

Commander/Director
US Army Cold Regions Research
& Engineering Laboratory
ATTN: CRREL-RG (Mr. George Aitken)
Hanover, NH 03755

Commander
US Army Cold Regions Research
& Engineering Laboratory
ATTN: CRREL-RG (Mr. Roger H. Berger)
Hanover, NH 03755

Commander
US Army Armament Research
& Development Command
ATTN: DRDAR-AC (Mr. James Greenfield)
Dover, NJ 07801

Commander
US Army Armament Research
& Development Command
ATTN: DRDAR-TSS (Bldg #59)
Dover, NJ 07801

Commander
US Army Armament Research
& Development Command
ATTN: DRCPM-CAWS-EI (Mr. Peteris Jansons)
Dover, NJ 07801

Commander
US Army Armament Research
& Development Command
ATTN: DRCPM-CAWS-EI (Mr. G. H. Waldron)
Dover, NJ 07801

Deputy Joint Project Manager
for Navy/USMC SAL GP
ATTN: DRCPM-CAWS-NV (CPT Joseph Miceli)
Dover, NJ 07801

Commander/Director
US Army Combat Surveillance & Target
Acquisition Laboratory
ATTN: DELCS-I (Mr. David Longinotti)
Fort Monmouth, NJ 07703

Commander/Director
US Army Combat Surveillance & Target
Acquisition Laboratory
ATTN: DELCS-PE (Mr. Ben A. Di Campi)
Fort Monmouth, NJ 07703

Commander/Director
US Army Combat Surveillance & Target
Acquisition Laboratory
ATTN: DELCS-R-S (Mr. Donald L. Fofani)
Fort Monmouth, NJ 07703

Director
US Army Electronics Technology &
Devices Laboratory
ATTN: DELET-DD (S. Danko)
Fort Monmouth, NJ 07703

Project Manager
FIREFINDER/REMBASS
ATTN: DRCPM-FFR-TM (Mr. John M. Bialo)
Fort Monmouth, NJ 07703

Commander
US Army Electronics Research
& Development Command
ATTN: DRDEL-SA (Dr. Walter S. McAfee)
Fort Monmouth, NJ 07703

OLA, 2WS (MAC)
Holloman AFB, NM 88330
Commander
Air Force Weapons Laboratory
ATTN: AFWL/WE (MAJ John R. Elrick)
Kirtland, AFB, NM 87117

Director
USA TRADOC Systems Analysis Activity
ATTN: ATAA-SL
White Sands Missile Range, NM 88002

Director
USA TRADOC Systems Analysis Activity
ATTN: ATAA-SL (Dolores Anguiano)
White Sands Missile Range, NM 88002

Director
USA TRADOC Systems Analysis Activity
ATTN: ATAA-TDB (Mr. Louie Dominguez)
White Sands Missile Range, NM 88002

Director
USA TRADOC Systems Analysis Activity
ATTN: ATAA-TDB (Mr. William J. Leach)
White Sands Missile Range, NM 88002

Director
USA TRADOC Systems Analysis Activity
ATTN: ATAA-TGP (Mr. Roger F. Willis)
White Sands Missile Range, NM 88002

Director
Office of Missile Electronic Warfare
ATTN: DELEW-M-STO (Dr. Steven Kovel)
White Sands Missile Range, NM 88002

Office of the Test Director
Joint Services EO GW CM Test Program
ATTN: DRXDE-TD (Mr. Weldon Findley)
White Sands Missile Range, NM 88002

Commander
US Army White Sands Missile Range
ATTN: STEWS-PT-AL (Laurel B. Saunders)
White Sands Missile Range, NM 88002

Commander
US Army R&D Coordinator
US Embassy - Bonn
Box 165
APO New York 09080

Grumman Aerospace Corporation
Research Department - MS A08-35
ATTN: John E. A. Selby
Bethpage, NY 11714

Rome Air Development Center
ATTN: Documents Library
TSLD (Bette Smith)
Griffiss AFB, NY 13441

Dr. Roberto Vaglio-Laurin
Faculty of Arts and Science
Dept. of Applied Science
26-36 Stuyvesant Street
New York, NY 10003

Air Force Wright Aeronautical Laboratories/
Avionics Laboratory
ATTN: AFWAL/AARI-3 (Mr. Harold Geltmacher)
Wright-Patterson AFB, OH 45433

Air Force Wright Aeronautical Laboratories/
Avionics Laboratory
ATTN: AFWAL/AARI-3 (CPT William C. Smith)
Wright-Patterson AFB, OH 45433

Commandant
US Army Field Artillery School
ATTN: ATSF-CF-R (CPT James M. Watson)
Fort Sill, OK 73503

Commandant
US Army Field Artillery School
ATTN: ATSF-CD-MS
Fort Sill, OK 73503

Commandant
US Army Field Artillery School
ATTN: ATSF-CF-R
Fort Sill, OK 73503

Commandant
US Army Field Artillery School
ATTN: NOAA Liaison Officer
(CDR Jeffrey G. Carlen)
Fort Sill, OK 73503

Commandant
US Army Field Artillery School
Morris Swett Library
ATTN: Reference Librarian
Fort Sill, OK 73503

Commander
Naval Air Development Center
ATTN: Code 301 (Mr. George F. Eck)
Warminster, PA 18974

The University of Texas at El Paso
Electrical Engineering Department
ATTN: Dr. Joseph H. Pierluissi
El Paso, TX 79968

Commandant
US Army Air Defense School
ATTN: ATSA-CD-SC-A (CPT Charles T. Thorn)
Fort Bliss, TX 79916

Commander
HQ, TRADOC Combined Arms Test Activity
ATTN: ATCAT-OP-Q (CPT Henry C. Cobb, Jr.)
Fort Hood, TX 76544

Commander
HQ, TRADOC Combined Arms Test Activity
ATTN: ATCAT-SCI (Dr. Darrell W. Collier)
Fort Hood, TX 76544

Commander
US Army Dugway Proving Ground
ATTN: STEDP-MT-DA-L
Dugway, UT 84022

Commander
US Army Dugway Proving Ground
ATTN: STEDP-MT-DA-M (Mr. Paul E. Carlson)
Dugway, UT 84022

Commander
US Army Dugway Proving Ground
ATTN: STEDP-MT-DA-T (Mr. John Trethewey)
Dugway, UT 84022

Commander
US Army Dugway Proving Ground
ATTN: STEDP-MT-DA-T (Mr. William Peterson)
Dugway, UT 84022

Defense Documentation Center
ATTN: DDC-TCA
Cameron Station Bldg 5
Alexandria, VA 22314
12

Ballistic Missile Defense Program Office
ATTN: DACS-BMT (Colonel Harry F. Ennis)
5001 Eisenhower Avenue
Alexandria, VA 22333

Defense Technical Information Center
ATTN: DDA-2 (Mr. James E. Shafer)
Cameron Station, Bldg 5
Alexandria, VA 22314

Commander
US Army Materiel Development
& Readiness Command
ATTN: DRCBSI-EE (Mr. Albert Giambalvo)
5001 Eisenhower Avenue
Alexandria, VA 22333

Commander
US Army Materiel Development
& Readiness Command
ATTN: DRCLDC (Mr. James Bender)
5001 Eisenhower Avenue
Alexandria, VA 22333

Defense Advanced Rsch Projects Agency
ATTN: Steve Zakanyez
1400 Wilson Blvd
Arlington, VA 22209

Defense Advanced Rsch Projects Agency
ATTN: Dr. James Tegnelia
1400 Wilson Blvd
Arlington, VA 22209

Institute for Defense Analyses
ATTN: Mr. Lucien M. Biberman
400 Army-Navy Drive
Arlington, VA 22202

Institute for Defense Analyses
ATTN: Dr. Ernest Bauer
400 Army-Navy Drive
Arlington, VA 22202

Institute for Defense Analyses
ATTN: Dr. Hans G. Wolfhard
400 Army-Navy Drive
Arlington, VA 22202

System Planning Corporation
ATTN: Mr. Daniel Friedman
1500 Wilson Boulevard
Arlington, VA 22209

System Planning Corporation
ATTN: COL Hank Shelton
1500 Wilson Boulevard
Arlington, VA 22209

US Army Intelligence & Security Command
ATTN: Edwin Speakman, Scientific Advisor
Arlington Hall Station
Arlington, VA 22212

Commander
US Army Operational Test
& Evaluation Agency
ATTN: CSTE-ED (Mr. Floyd I. Hill)
5600 Columbia Pike
Falls Church, VA 22041

Commander and Director
US Army Engineer Topographic Laboratories
ATTN: ETL-GS-A (Mr. Thomas Neidringhaus)
Fort Belvoir, VA 22060

Director
US Army Night Vision &
Electro-Optics Laboratory
ATTN: DELNV-L (Dr. Rudolf G. Buser)
Fort Belvoir, VA 22060

Director
US Army Night Vision &
Electro-Optics Laboratory
ATTN: DELNV-L (Dr. Robert S. Rodhe)
Fort Belvoir, VA 22060

Director
US Army Night Vision &
Electro-Optics Laboratory
ATTN: DELNV-VI (Mr. Joseph R. Moulton)
Fort Belvoir, VA 22060

Director
US Army Night Vision &
Electro-Optics Laboratory
ATTN: DELNV-VI (Luanne P. Obert)
Fort Belvoir, VA 22060

Director
US Army Night Vision
& Electro-Optics Laboratory
ATTN: DELNV-VI (Mr. Thomas W. Cassidy)
Fort Belvoir, VA 22060

Director
US Army Night Vision &
Electro-Optics Laboratory
ATTN: DELNV-VI (Mr. Richard J. Bergemann)
Fort Belvoir, VA 22060

Director
US Army Night Vision &
Electro-Optics Laboratory
ATTN: DELNV-VI (Dr. James A. Ratches)
Fort Belvoir, VA 22060

Commander
US Army Training & Doctrine Command
ATTN: ATCD-AN
Fort Monroe, VA 23651

Commander
US Army Training & Doctrine Command
ATTN: ATCD-AN-M
Fort Monroe, VA 23651

Commander
US Army Training & Doctrine Command
ATTN: ATCD-F-A (Mr. Chris O'Connor, Jr.)
Fort Monroe, VA 23651

Commander
US Army Training & Doctrine Command
ATTN: ATCD-IE-R (Mr. David M. Ingram)
Fort Monroe, VA 23651

Commander
US Army Training & Doctrine Command
ATTN: ATCD-M-I/ATCD-M-A
Fort Monroe, VA 23651

Commander
US Army Training & Doctrine Command
ATTN: ATDOC-TA (Dr. Marvin P. Pastel)
Fort Monroe, VA 23651

Department of the Air Force
OL-I, AWS
Fort Monroe, VA 23651

Department of the Air Force
HQS 5 Weather Wing (MAC)
ATTN: 5 WW/DN
Langley Air Force Base, VA 23655

Commander
US Army INSCOM/Quest Research Corporation
ATTN: Mr. Donald Wilmot
6845 Elm Street, Suite 407
McLean, VA 22101

General Research Corporation
ATTN: Dr. Ralph Zirkind
7655 Old Springhouse Road
McLean, VA 22102

Science Applications, Inc.
8400 Westpark Drive
ATTN: Dr. John E. Cockayne
McLean, VA 22102

US Army Nuclear & Chemical Agency
ATTN: MONA-WE (Dr. John A. Berberet)
7500 Backlick Road, Bldg 2073
Springfield, VA 22150

Director
US Army Signals Warfare Laboratory
ATTN: DELSW-EA (Mr. Douglas Harkleroad)
Vint Hill Farms Station
Warrenton, VA 22186

Director
US Army Signals Warfare Laboratory
ATTN: DELSW-OS (Dr. Royal H. Burkhardt)
Vint Hill Farms Station
Warrenton, VA 22186

Commander
US Army Cold Regions Test Center
ATTN: STECR-TD (Mr. Jerold Barger)
APO Seattle, WA 98733

HQDA (SAUS-OR/Hunter M. Woodall, Jr./
Dr. Herbert K. Fallin)
Rm 2E 614, Pentagon
Washington, DC 20301

COL Elbert W. Friday, Jr.
OUSDRE
Rm 3D 129, Pentagon
Washington, DC 20301

Defense Communications Agency
Technical Library Center
Code 222
Washington, DC 20305

Director
Defense Nuclear Agency
ATTN: Technical Library (Mrs. Betty Fox)
Washington, DC 20305

Director
Defense Nuclear Agency
ATTN: RAAE (Dr. Carl Fitz)
Washington, DC 20305

Director
Defense Nuclear Agency
ATTN: SPAS (Mr. Donald J. Kohler)
Washington, DC 20305

Defense Intelligence Agency
ATTN: DT/AC (LTC Robert Poplawski)
Washington, DC 20301

HQDA (DAMA-ARZ-D/Dr. Verderame)
Washington, DC 20310

HQDA (DAMI-ISP/Mr. Beck)
Washington, DC 20310

Department of the Army
Deputy Chief of Staff for
Operations and Plans
ATTN: DAMO-RQ
Washington, DC 20310

Department of the Army
Director of Telecommunications and
Command and Control
ATTN: DAMO-TCZ
Washington, DC 20310

Department of the Army
Assistant Chief of Staff for Intelligence
ATTN: DAMI-TS
Washington, DC 20310

HQDA (DAEN-RDM/Dr. de Percin)
Casimir Pulaski Building
20 Massachusetts Avenue
Room 6203
Washington, DC 20314

National Science Foundation
Division of Atmospheric Sciences
ATTN: Dr. Eugene W. Bierly
1800 G. Street, N.W.
Washington, DC 20550

Director
Naval Research Laboratory
ATTN: Code 4320 (Dr. Lothar H. Ruhnke)
Washington, DC 20375

Commanding Officer
Naval Research Laboratory
ATTN: Code 6009 (Dr. John MacCallum, Jr.)
Washington, DC 20375

Commanding Officer
Naval Research Laboratory
ATTN: Code 6530 (Mr. Raymond A. Patten)
Washington, DC 20375

Commanding Officer
Naval Research Laboratory
ATTN: Code 6533 (Dr. James A. Dowling)
Washington, DC 20375

ATMOSPHERIC SCIENCES RESEARCH REPORTS

1. Lindberg, J. D. "An Improvement to a Method for Measuring the Absorption Coefficient of Atmospheric Dust and other Strongly Absorbing Powders," ECOM-5565, July 1975.
2. Avara, Elton P., "Mesoscale Wind Shears Derived from Thermal Winds," ECOM-5566, July 1975.
3. Gomez, Richard B., and Joseph H. Pierluissi, "Incomplete Gamma Function Approximation for King's Strong-Line Transmittance Model," ECOM-5567, July 1975.
4. Blanco, A. J., and B. F. Engebos, "Ballistic Wind Weighting Functions for Tank Projectiles," ECOM-5568, August 1975.
5. Taylor, Fredrick J., Jack Smith, and Thomas H. Pries, "Crosswind Measurements through Pattern Recognition Techniques," ECOM-5569, July 1975.
6. Walters, D. L., "Crosswind Weighting Functions for Direct-Fire Projectiles," ECOM-5570, August 1975.
7. Duncan, Louis D., "An Improved Algorithm for the Iterated Minimal Information Solution for Remote Sounding of Temperature," ECOM-5571, August 1975.
8. Robbiani, Raymond L., "Tactical Field Demonstration of Mobile Weather Radar Set AN/TPS-41 at Fort Rucker, Alabama," ECOM-5572, August 1975.
9. Miers, B., G. Blackman, D. Langer, and N. Lorimier, "Analysis of SMS/GOES Film Data," ECOM-5573, September 1975.
10. Manquero, Carlos, Louis Duncan, and Rufus Bruce, "An Indication from Satellite Measurements of Atmospheric CO₂ Variability," ECOM-5574, September 1975.
11. Petracca, Carmine, and James D. Lindberg, "Installation and Operation of an Atmospheric Particulate Collector," ECOM-5575, September 1975.
12. Avara, Elton P., and George Alexander, "Empirical Investigation of Three Iterative Methods for Inverting the Radiative Transfer Equation," ECOM-5576, October 1975.
13. Alexander, George D., "A Digital Data Acquisition Interface for the SMS Direct Readout Ground Station - Concept and Preliminary Design," ECOM-5577, October 1975.
14. Cantor, Israel, "Enhancement of Point Source Thermal Radiation Under Clouds in a Nonattenuating Medium," ECOM-5578, October 1975.

15. Norton, Colburn, and Glenn Hoidale, "The Diurnal Variation of Mixing Height by Month over White Sands Missile Range, NM," ECOM-5579, November 1975.
16. Avara, Elton P., "On the Spectrum Analysis of Binary Data," ECOM-5580, November 1975.
17. Taylor, Fredrick J., Thomas H. Pries, and Chao-Huan Huang, "Optimal Wind Velocity Estimation," ECOM-5581, December 1975.
18. Avara, Elton P., "Some Effects of Autocorrelated and Cross-Correlated Noise on the Analysis of Variance," ECOM-5582, December 1975.
19. Gillespie, Patti S., R. L. Armstrong, and Kenneth O. White, "The Spectral Characteristics and Atmospheric CO₂ Absorption of the Ho³:YLF Laser at 2.05 μ m," ECOM-5583, December 1975.
20. Novlan, David J., "An Empirical Method of Forecasting Thunderstorms for the White Sands Missile Range," ECOM-5584, February 1976.
21. Avara, Elton P., "Randomization Effects in Hypothesis Testing with Autocorrelated Noise," ECOM-5585, February 1976.
22. Watkins, Wendell R., "Improvements in Long Path Absorption Cell Measurement," ECOM-5586, March 1976.
23. Thomas, Joe, George D. Alexander, and Marvin Dubbin, "SATTEL - An Army Dedicated Meteorological Telemetry System," ECOM-5587, March 1976.
24. Kennedy, Bruce W., and Delbert Bynum, "Army User Test Program for the RDT&E-XM-75 Meteorological Rocket," ECOM-5588, April 1976.
25. Barnett, Kenneth M., "A Description of the Artillery Meteorological Comparisons at White Sands Missile Range, October 1974 - December 1974 ('PASS' - Prototype Artillery [Meteorological] Subsystem)," ECOM-5589, April 1976.
26. Miller, Walter B., "Preliminary Analysis of Fall-of-Shot From Project 'PASS'," ECOM-5590, April 1976.
27. Avara, Elton P., "Error Analysis of Minimum Information and Smith's Direct Methods for Inverting the Radiative Transfer Equation," ECOM-5591, April 1976.
28. Yee, Young P., James D. Horn, and George Alexander, "Synoptic Thermal Wind Calculations from Radiosonde Observations Over the Southwestern United States," ECOM-5592, May 1976.

29. Duncan, Louis D., and Mary Ann Seagraves, "Applications of Empirical Corrections to NOAA-4 VTPR Observations," ECOM-5593, May 1976.
30. Miers, Bruce T., and Steve Weaver, "Applications of Meteorological Satellite Data to Weather Sensitive Army Operations," ECOM-5594, May 1976.
31. Sharenow, Moses, "Redesign and Improvement of Balloon ML-566," ECOM-5595, June 1976.
32. Hansen, Frank V., "The Depth of the Surface Boundary Layer," ECOM-5596, June 1976.
33. Pinnick, R. G., and E. B. Stenmark, "Response Calculations for a Commercial Light-Scattering Aerosol Counter," ECOM-5597, July 1976.
34. Mason, J., and G. B. Hoidale, "Visibility as an Estimator of Infrared Transmittance," ECOM-5598, July 1976.
35. Bruce, Rufus E., Louis D. Duncan, and Joseph H. Pierluissi, "Experimental Study of the Relationship Between Radiosonde Temperatures and Radiometric-Area Temperatures," ECOM-5599, August 1976.
36. Duncan, Louis D., "Stratospheric Wind Shear Computed from Satellite Thermal Sounder Measurements," ECOM-5800, September 1976.
37. Taylor, F., P. Mohan, P. Joseph, and T. Pries, "An All Digital Automated Wind Measurement System," ECOM-5801, September 1976.
38. Bruce, Charles, "Development of Spectrophones for CW and Pulsed Radiation Sources," ECOM-5802, September 1976.
39. Duncan, Louis D., and Mary Ann Seagraves, "Another Method for Estimating Clear Column Radiances," ECOM-5803, October 1976.
40. Blanco, Abel J., and Larry E. Taylor, "Artillery Meteorological Analysis of Project Pass," ECOM-5804, October 1976.
41. Miller, Walter, and Bernard Engebos, "A Mathematical Structure for Refinement of Sound Ranging Estimates," ECOM-5805, November 1976.
42. Gillespie, James B., and James D. Lindberg, "A Method to Obtain Diffuse Reflectance Measurements from 1.0 and 3.0 μ m Using a Cary 17I Spectrophotometer," ECOM-5806, November 1976.
43. Rubio, Roberto, and Robert O. Olsen, "A Study of the Effects of Temperature Variations on Radio Wave Absorption," ECOM-5807, November 1976.

44. Ballard, Harold N., "Temperature Measurements in the Stratosphere from Balloon-Borne Instrument Platforms, 1968-1975," ECOM-5808, December 1976.
45. Monahan, H. H., "An Approach to the Short-Range Prediction of Early Morning Radiation Fog," ECOM-5809, January 1977.
46. Engebos, Bernard Francis, "Introduction to Multiple State Multiple Action Decision Theory and Its Relation to Mixing Structures," ECOM-5810, January 1977.
47. Low, Richard D. H., "Effects of Cloud Particles on Remote Sensing from Space in the 10-Micrometer Infrared Region," ECOM-5811, January 1977.
48. Bonner, Robert S., and R. Newton, "Application of the AN/GVS-5 Laser Rangefinder to Cloud Base Height Measurements," ECOM-5812, February 1977.
49. Rubio, Roberto, "Lidar Detection of Subvisible Reentry Vehicle Erosive Atmospheric Material," ECOM-5813, March 1977.
50. Low, Richard D. H., and J. D. Horn, "Mesoscale Determination of Cloud-Top Height: Problems and Solutions," ECOM-5814, March 1977.
51. Duncan, Louis D., and Mary Ann Seagraves, "Evaluation of the NOAA-4 VTPR Thermal Winds for Nuclear Fallout Predictions," ECOM-5815, March 1977.
52. Randhawa, Jagir S., M. Izquierdo, Carlos McDonald, and Zvi Salpeter, "Stratospheric Ozone Density as Measured by a Chemiluminescent Sensor During the Stratcom VI-A Flight," ECOM-5816, April 1977.
53. Rubio, Roberto, and Mike Izquierdo, "Measurements of Net Atmospheric Irradiance in the 0.7- to 2.8-Micrometer Infrared Region," ECOM-5817, May 1977.
54. Ballard, Harold N., Jose M. Serna, and Frank P. Hudson, Consultant for Chemical Kinetics, "Calculation of Selected Atmospheric Composition Parameters for the Mid-Latitude, September Stratosphere," ECOM-5818, May 1977.
55. Mitchell, J. D., R. S. Sagar, and R. O. Olsen, "Positive Ions in the Middle Atmosphere During Sunrise Conditions," ECOM-5819, May 1977.
56. White, Kenneth O., Wendell R. Watkins, Stuart A. Schleusener, and Ronald L. Johnson, "Solid-State Laser Wavelength Identification Using a Reference Absorber," ECOM-5820, June 1977.
57. Watkins, Wendell R., and Richard G. Dixon, "Automation of Long-Path Absorption Cell Measurements," ECOM-5821, June 1977.

58. Taylor, S. E., J. M. Davis, and J. B. Mason, "Analysis of Observed Soil Skin Moisture Effects on Reflectance," ECOM-5822, June 1977.
59. Duncan, Louis D., and Mary Ann Seagraves, "Fallout Predictions Computed from Satellite Derived Winds," ECOM-5823, June 1977.
60. Snider, D. E., D. G. Murcray, F. H. Murcray, and W. J. Williams, "Investigation of High-Altitude Enhanced Infrared Background Emissions," (U), SECRET, ECOM-5824, June 1977.
61. Dubbin, Marvin H., and Dennis Hall, "Synchronous Meteorological Satellite Direct Readout Ground System Digital Video Electronics," ECOM-5825, June 1977.
62. Miller, W., and B. Engebos, "A Preliminary Analysis of Two Sound Ranging Algorithms," ECOM-5826, July 1977.
63. Kennedy, Bruce W., and James K. Luers, "Ballistic Sphere Techniques for Measuring Atmospheric Parameters," ECOM-5827, July 1977.
64. Duncan, Louis D., "Zenith Angle Variation of Satellite Thermal Sounder Measurements," ECOM-5828, August 1977.
65. Hansen, Frank V., "The Critical Richardson Number," ECOM-5829, September 1977.
66. Ballard, Harold N., and Frank P. Hudson (Compilers), "Stratospheric Composition Balloon-Borne Experiment," ECOM-5830, October 1977.
67. Barr, William C., and Arnold C. Peterson, "Wind Measuring Accuracy Test of Meteorological Systems," ECOM-5831, November 1977.
68. Ethridge, G. A., and F. V. Hansen, "Atmospheric Diffusion: Similarity Theory and Empirical Derivations for Use in Boundary Layer Diffusion Problems," ECOM-5832, November 1977.
69. Low, Richard D. H., "The Internal Cloud Radiation Field and a Technique for Determining Cloud Blackness," ECOM-5833, December 1977.
70. Watkins, Wendell R., Kenneth O. White, Charles W. Bruce, Donald L. Walters, and James D. Lindberg, "Measurements Required for Prediction of High Energy Laser Transmission," ECOM-5834, December 1977.
71. Rubio, Robert, "Investigation of Abrupt Decreases in Atmospherically Backscattered Laser Energy," ECOM-5835, December 1977.
72. Monahan, H. H., and R. M. Cionco, "An Interpretative Review of Existing Capabilities for Measuring and Forecasting Selected Weather Variables (Emphasizing Remote Means)," ASL-TR-0001, January 1978.

73. Heaps, Melvin G., "The 1979 Solar Eclipse and Validation of D-Region Models," ASL-TR-0002, March 1978.
74. Jennings, S. G., and J. R. Gillespie, "M.I.E. Theory Sensitivity Studies - The Effects of Aerosol Complex Refractive Index and Size Distribution Variations on Extinction and Absorption Coefficients, Part II: Analysis of the Computational Results," ASL-TR-0003, March 1978.
75. White, Kenneth O., et al, "Water Vapor Continuum Absorption in the 3.5 μ m to 4.0 μ m Region," ASL-TR-0004, March 1978.
76. Olsen, Robert O., and Bruce W. Kennedy, "ABRES Pretest Atmospheric Measurements," ASL-TR-0005, April 1978.
77. Ballard, Harold N., Jose M. Serna, and Frank P. Hudson, "Calculation of Atmospheric Composition in the High Latitude September Stratosphere," ASL-TR-0006, May 1978.
78. Watkins, Wendell R., et al, "Water Vapor Absorption Coefficients at HF Laser Wavelengths," ASL-TR-0007, May 1978.
79. Hansen, Frank V., "The Growth and Prediction of Nocturnal Inversions," ASL-TR-0008, May 1978.
80. Samuel, Christine, Charles Bruce, and Ralph Brewer, "Spectrophone Analysis of Gas Samples Obtained at Field Site," ASL-TR-0009, June 1978.
81. Pinnick, R. G., et al., "Vertical Structure in Atmospheric Fog and Haze and its Effects on IR Extinction," ASL-TR-0010, July 1978.
82. Low, Richard D. H., Louis D. Duncan, and Richard B. Gomez, "The Microphysical Basis of Fog Optical Characterization," ASL-TR-0011, August 1978.
83. Heaps, Melvin G., "The Effect of a Solar Proton Event on the Minor Neutral Constituents of the Summer Polar Mesosphere," ASL-TR-0012, August 1978.
84. Mason, James B., "Light Attenuation in Falling Snow," ASL-TR-0013, August 1978.
85. Blanco, Abel J., "Long-Range Artillery Sound Ranging: 'PASS' Meteorological Application," ASL-TR-0014, September 1978.
86. Heaps, M. G., and F. E. Niles, "Modeling of Ion Chemistry of the D-Region: A Case Study Based Upon the 1966 Total Solar Eclipse," ASL-TR-0015, September 1978.

87. Jennings, S. G., and R. G. Pinnick, "Effects of Particulate Complex Refractive Index and Particle Size Distribution Variations on Atmospheric Extinction and Absorption for Visible Through Middle-Infrared Wavelengths," ASL-TR-0016, September 1978.
88. Watkins, Wendell R., Kenneth O. White, Lanny R. Bower, and Brian Z. Sojka, "Pressure Dependence of the Water Vapor Continuum Absorption in the 3.5- to 4.0-Micrometer Region," ASL-TR-0017, September 1978.
89. Miller, W. B., and B. F. Engebos, "Behavior of Four Sound Ranging Techniques in an Idealized Physical Environment," ASL-TR-0018, September 1978.
90. Gomez, Richard G., "Effectiveness Studies of the CBU-88/B Bomb, Cluster, Smoke Weapon," (U), CONFIDENTIAL ASL-TR-0019, September 1978.
91. Miller, August, Richard C. Shirkey, and Mary Ann Seagraves, "Calculation of Thermal Emission from Aerosols Using the Doubling Technique," ASL-TR-0020, November 1978.
92. Lindberg, James D., et al, "Measured Effects of Battlefield Dust and Smoke on Visible, Infrared, and Millimeter Wavelengths Propagation: A Preliminary Report on Dusty Infrared Test-I (DIRT-I)," ASL-TR-0021, January 1979.
93. Kennedy, Bruce W., Arthur Kinghorn, and B. R. Hixon, "Engineering Flight Tests of Range Meteorological Sounding System Radiosonde," ASL-TR-0022, February 1979.
94. Rubio, Roberto, and Don Hoock, "Microwave Effective Earth Radius Factor Variability at Wiesbaden and Balboa," ASL-TR-0023, February 1979.
95. Low, Richard D. H., "A Theoretical Investigation of Cloud/Fog Optical Properties and Their Spectral Correlations," ASL-TR-0024, February 1979.
96. Pinnick, R. G., and H. J. Auvermann, "Response Characteristics of Knollenberg Light-Scattering Aerosol Counters," ASL-TR-0025, February 1979.
97. Heaps, Melvin G., Robert O. Olsen, and Warren W. Berning, "Solar Eclipse 1979, Atmospheric Sciences Laboratory Program Overview," ASL-TR-0026, February 1979.
98. Blanco, Abel J., "Long-Range Artillery Sound Ranging: 'PASS' GR-8 Sound Ranging Data," ASL-TR-0027, March 1979.
99. Kennedy, Bruce W., and Jose M. Serna, "Meteorological Rocket Network System Reliability," ASL-TR-0028, March 1979.

100. Swingle, Donald M., "Effects of Arrival Time Errors in Weighted Range Equation Solutions for Linear Base Sound Ranging," ASL-TR-0029, April 1979.
101. Umstead, Robert K., Ricardo Pena, and Frank V. Hansen, "KWIK: An Algorithm for Calculating Munition Expenditures for Smoke Screening/Obscuration in Tactical Situations," ASL-TR-0030, April 1979.
102. D'Arcy, Edward M., "Accuracy Validation of the Modified Nike Hercules Radar," ASL-TR-0031, May 1979.
103. Rodriguez, Ruben, "Evaluation of the Passive Remote Crosswind Sensor," ASL-TR-0032, May 1979.
104. Barber, T. L., and R. Rodriguez, "Transit Time Lidar Measurement of Near-Surface Winds in the Atmosphere," ASL-TR-0033, May 1979.
105. Low, Richard D. H., Louis D. Duncan, and Y. Y. Roger R. Hsiao, "Micro-physical and Optical Properties of California Coastal Fogs at Fort Ord," ASL-TR-0034, June 1979.
106. Rodriguez, Ruben, and William J. Vechione, "Evaluation of the Saturation Resistant Crosswind Sensor," ASL-TR-0035, July 1979.
107. Ohmstede, William D., "The Dynamics of Material Layers," ASL-TR-0036, July 1979.
108. Pinnick, R. G., S. G. Jennings, Petr Chylek, and H. J. Auvermann, "Relationships between IR Extinction Absorption, and Liquid Water Content of Fogs," ASL-TR-0037, August 1979.
109. Rodriguez, Ruben, and William J. Vechione, "Performance Evaluation of the Optical Crosswind Profiler," ASL-TR-0038, August 1979.
110. Miers, Bruce T., "Precipitation Estimation Using Satellite Data," ASL-TR-0039, September 1979.
111. Dickson, David H., and Charles M. Sonnenschein, "Helicopter Remote Wind Sensor System Description," ASL-TR-0040, September 1979.
112. Heaps, Melvin G., and Joseph M. Heimerl, "Validation of the Dairchem Code, I: Quiet Midlatitude Conditions," ASL-TR-0041, September 1979.
113. Bonner, Robert S., and William J. Lentz, "The Visioceilometer: A Portable Cloud Height and Visibility Indicator," ASL-TR-0042, October 1979.
114. Cohn, Stephen L., "The Role of Atmospheric Sulfates in Battlefield Obscurations," ASL-TR-0043, October 1979.

115. Fawbush, E. J., et al, "Characterization of Atmospheric Conditions at the High Energy Laser System Test Facility (HELSTF), White Sands Missile Range, New Mexico, Part I, 24 March to 8 April 1977," ASL-TR-0044, November 1979.
116. Barber, Ted L., "Short-Time Mass Variation in Natural Atmospheric Dust," ASL-TR-0045, November 1979.
117. Low, Richard D. H., "Fog Evolution in the Visible and Infrared Spectral Regions and its Meaning in Optical Modeling," ASL-TR-0046, December 1979.
118. Duncan, Louis D., et al, "The Electro-Optical Systems Atmospheric Effects Library, Volume I: Technical Documentation," ASL-TR-0047, December 1979.
119. Shirkey, R. C., et al, "Interim E-0 SAEL, Volume II, Users Manual," ASL-TR-0048, December 1979.
120. Kobayashi, H. K., "Atmospheric Effects on Millimeter Radio Waves," ASL-TR-0049, January 1980.
121. Seagraves, Mary Ann, and Louis D. Duncan, "An Analysis of Transmittances Measured Through Battlefield Dust Clouds," ASL-TR-0050, February 1980.
122. Dickson, David H., and Jon E. Ottesen, "Helicopter Remote Wind Sensor Flight Test," ASL-TR-0051, February 1980.
123. Pinnick, R. G., and S. G. Jennings, "Relationships Between Radiative Properties and Mass Content of Phosphoric Acid, HC, Petroleum Oil, and Sulfuric Acid Military Smokes," ASL-TR-0052, April 1980.
124. Hinds, B. D., and J. B. Gillespie, "Optical Characterization of Atmospheric Particulates on San Nicolas Island, California," ASL-TR-0053, April 1980.
125. Miers, Bruce T., "Precipitation Estimation for Military Hydrology," ASL-TR-0054, April 1980.
126. Stenmark, Ernest B., "Objective Quality Control of Artillery Computer Meteorological Messages," ASL-TR-0055, April 1980.
127. Duncan, Louis D., and Richard D. H. Low, "Bimodal Size Distribution Models for Fogs at Meppen, Germany," ASL-TR-0056, April 1980.
128. Olsen, Robert O., and Jagir S. Randhawa, "The Influence of Atmospheric Dynamics on Ozone and Temperature Structure," ASL-TR-0057, May 1980.

129. Kennedy, Bruce W., et al, "Dusty Infrared Test-II (DIRT-II) Program," ASL-TR-0058, May 1980.
130. Heaps, Melvin G., Robert O. Olsen, Warren Berning, John Cross, and Arthur Gilcrease, "1979 Solar Eclipse, Part I - Atmospheric Sciences Laboratory Field Program Summary," ASL-TR-0059, May 1980
131. Miller, Walter B., "User's Guide for Passive Target Acquisition Program Two (PTAP-2)," ASL-TR-0060, June 1980.
132. Holt, E. H., editor, "Atmospheric Data Requirements for Battlefield Obscuration Applications," ASL-TR-0061, June 1980.
133. Shirkey, Richard C., August Miller, George H. Goedecke, and Yugal Behl, "Single Scattering Code AGAUSX: Theory, Applications, Comparisons, and Listing," ASL-TR-0062, July 1980.
134. Sojka, Brian Z., and Kenneth O. White, "Evaluation of Specialized Photoacoustic Absorption Chambers for Near-Millimeter Wave (NMMW) Propagation Measurements," ASL-TR-0063, August 1980.
135. Bruce, Charles W., Young Paul Yee, and S. G. Jennings, "In Situ Measurement of the Ratio of Aerosol Absorption to Extinction Coefficient," ASL-TR-0064, August 1980.
136. Yee, Young Paul, Charles W. Bruce, and Ralph J. Brewer, "Gaseous/Particulate Absorption Studies at WSMR using Laser Sourced Spectrophones," ASL-TR-0065, June 1980.
137. Lindberg, James D., Radon B. Loveland, Melvin Heaps, James B. Gillespie, and Andrew F. Lewis, "Battlefield Dust and Atmospheric Characterization Measurements During West German Summertime Conditions in Support of Grafenwohr Tests," ASL-TR-0066, September 1980.
138. Vechione, W. J., "Evaluation of the Environmental Instruments, Incorporated Series 200 Dual Component Wind Set," ASL-TR-0067, September 1980.
139. Bruce, C. W., Y. P. Yee, B. D. Hinds, R. G. Pinnick, R. J. Brewer, and J. Minjares, "Initial Field Measurements of Atmospheric Absorption at 9 μ m to 11 μ m Wavelengths," ASL-TR-0068, October 1980.
140. Heaps, M. G., R. O. Olsen, K. D. Baker, D. A. Burt, L. C. Howlett, L. L. Jensen, E. F. Pound, and G. D. Allred, "1979 Solar Eclipse: Part II Initial Results for Ionization Sources, Electron Density, and Minor Neutral Constituents," ASL-TR-0069, October 1980.
141. Low, Richard D. H., "One-Dimensional Cloud Microphysical Models for Central Europe and their Optical Properties," ASL-TR-0070, October 1980.

142. Duncan, Louis D., James D. Lindberg, and Radon B. Loveland, "An Empirical Model of the Vertical Structure of German Fogs," ASL-TR-0071, November 1980.
143. Duncan, Louis D., "EOSAEL 80, Volume I, Technical Documentation," ASL-TR-0072, January 1981.
144. Shirkey, R. C., and S. G. O'Brien, "EOSAEL 80, Volume II, Users Manual," ASL-TR-0073, January 1981.
145. Bruce, C. W., "Characterization of Aerosol Nonlinear Effects on a High-Power CO₂ Laser Beam," ASL-TR-0074, February 1981.
146. Duncan, Louis D., and James D. Lindberg, "Air Mass Considerations in Fog Optical Modeling," ASL-TR-0075, February 1981.
147. Kunkel, Kenneth E., "Evaluation of a Tethered Kite Anemometer," ASL-TR-0076, February 1981.
148. Kunkel, K. E., et al, "Characterization of Atmospheric Conditions at the High Energy Laser System Test Facility (HELSTF) White Sands Missile Range, New Mexico, August 1977 to October 1978, Part II, Optical Turbulence, Wind, Water Vapor Pressure, Temperature," ASL-TR-0077, February 1981.
149. Miers, Bruce T., "Weather Scenarios for Central Germany," ASL-TR-0078, February 1981.
150. Cogan, James L., "Sensitivity Analysis of a Mesoscale Moisture Model," ASL-TR-0079, March 1981.
151. Brewer, R. J., C. W. Bruce, and J. L. Mater, "Optoacoustic Spectroscopy of C₂H₂ at the 9 μ m and 10 μ m C¹²O₂ Laser Wavelengths," ASL-TR-0080, March 1981.
152. Swingle, Donald M., "Reducible Errors in the Artillery Sound Ranging Solution, Part I: The Curvature Correction" (U), SECRET, ASL-TR-0081, April 1981.
153. Miller, Walter B., "The Existence and Implications of a Fundamental System of Linear Equations in Sound Ranging" (U), SECRET, ASL-TR-0082, April 1981.
154. Bruce, Dorothy, Charles W. Bruce, and Young Paul Yee, "Experimentally Determined Relationship Between Extinction and Liquid Water Content," ASL-TR-0083, April 1981.
155. Seagraves, Mary Ann, "Visible and Infrared Obscuration Effects of Ice Fog," ASL-TR-0084, May 1981.

156. Watkins, Wendell R., and Kenneth O. White, "Wedge Absorption Remote Sensor," ASL-TR-0085, May 1981.
157. Watkins, Wendell R., Kenneth O. White, and Laura J. Crow, "Turbulence Effects on Open Air Multipaths," ASL-TR-0086, May 1981.
158. Blanco, Abel J., "Extending Application of the Artillery Computer Meteorological Message," ASL-TR-0087, May 1981.
159. Heaps, M. G., D. W. Hoock, R. O. Olsen, B. F. Engebos, and R. Rubio, "High Frequency Position Location: An Assessment of Limitations and Potential Improvements," ASL-TR-0088, May 1981.
160. Watkins, Wendell R., and Kenneth O. White, "Laboratory Facility for Measurement of Hot Gaseous Plume Radiative Transfer," ASL-TR-0089, June 1981.
161. Heaps, M. G., "Dust Cloud Models: Sensitivity of Calculated Transmittances to Variations in Input Parameters," ASL-TR-0090, June 1981.
162. Seagraves, Mary Ann, "Some Optical Properties of Blowing Snow," ASL-TR-0091, June 1981.
163. Kobayashi, Herbert K., "Effect of Hail, Snow, and Melting Hydrometeors on Millimeter Radio Waves," ASL-TR-0092, July 1981.
164. Cogan, James L., "Techniques for the Computation of Wind, Ceiling, and Extinction Coefficient Using Currently Acquired RPV Data," ASL-TR-0093, July 1981.
165. Miller, Walter B., and Bernard F. Engebos, "On the Possibility of Improved Estimates for Effective Wind and Temperature," (U), SECRET, ASL-TR-0094, August 1981.
166. Heaps, Melvin G., "The Effect of Ionospheric Variability on the Accuracy of High Frequency Position Location," ASL-TR-0095, August 1981.
167. Sutherland, Robert A., Donald W. Hoock, and Richard B. Gomez, "An Objective Summary of US Army Electro-Optical Modeling and Field Testing in an Obscuring Environment," ASL-TR-0096, October 1981.
168. Pinnick, R. G., et al, "Backscatter and Extinction in Water Clouds," ASL-TR-0097, October 1981.
169. Cole, Henry P., and Melvin G. Heaps, "Properties of Dust as an Electron and Ion Attachment Site for Use in D Region Ion Chemistry," ASL-TR-0098, October 1981.

1. Spellicy, Robert L., Laura J. Crow, and Kenneth O. White, "Water Vapor Absorption Coefficients at HF Laser Wavelengths Part II: Development of the Measurement System and Measurements at Simulated Altitudes to 10 KM," ASL-TR-0099, November 1981.
2. Cohn, Stephen L., "Transport and Diffusion Solutions for Obscuration Using the XM-825 Smoke Munition," ASL-TR-0100, November 1981.
3. Pinnick, R. G., D. M. Garvey, and L. D. Duncan, "Calibration of Knollenberg FSSP Light-Scattering Counters for Measurement of Cloud Droplets," ASL-TR-0101, December 1981.
4. Cohn, Stephen L. and Ricardo Pena, "Munition Expenditure Model Verification: KWIK Phase I," ASL-TR-0102, December 1981.
5. Blackman, George R., "Cloud Geometry Analysis of the Smoke Week III Obscuration Trials," ASL-TR-0103, January 1982.
6. Sutherland, R. A., and D. W. Hoock, "An Improved Smoke Obscuration Model ACT II: Part 1 Theory," ASL-TR-0104, January 1982.

